

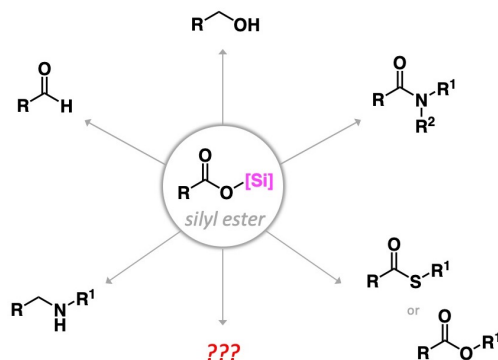
# Silyl Esters as Reactive Intermediates in Organic Synthesis

Melissa C. D'Amaral<sup>a</sup>  
Keith Andrews<sup>b</sup>  
Ross Denton<sup>b</sup>  
Marc J. Adler\*<sup>a</sup>

<sup>a</sup> Department of Chemistry & Biology, Toronto Metropolitan University, 350 Victoria Street, Toronto, ON, M5B 2K3, Canada.

<sup>b</sup> School of Chemistry, University of Nottingham, University Park Nottingham, NG7 2RD, United Kingdom.

marcjadler@torontomu.ca



Received:

Accepted:

Published online:

DOI:

Silyl esters have been exploited as meta-stable reaction intermediates – both purposefully and unintentionally – since at least the 1960s. Their reactivity is broadly related to the substituents on the silicon, and in this way their properties can be readily modulated. Silyl esters have unique reactivity profiles that have been used to generate downstream products of a range of functionalities, and because of this many excellent methods for the synthesis of a variety of value-added chemicals have been developed. Furthermore, because of the frequent use of hydrosilanes as terminal reductants in catalytic processes, silyl ester intermediates are likely more commonly utilized by synthetic chemists than currently realized. This review comprehensively summarizes the reactions known to take advantage of reactive silyl ester intermediates and discusses examples of catalytic reactions that proceed in an unanticipated manner through silyl ester intermediates.

1	Introduction	
2	Synthesis of Silyl Esters	
3	Making Amides from Silyl Esters	
3.1	Amidation using Chlorosilanes	
3.2	Amidation using Azasilanes	
3.3	Amidation using Oxysilanes	
3.4	Amidation using Hydrosilanes	
3.5	Amine Formation <i>via</i> Amidation/Reduction	
3.6	Miscellaneous	
4	Mechanistic Investigations of Amidation	
4.1	Mechanism of Amidation using Chlorosilanes	
4.2	Mechanism of Amidation using Hydrosilanes	
4.3	Mechanism of Amidation using Oxy-/Azasilanes	
5	Making Esters from Silyl Esters	
6	Making Aldehydes, Alcohols, Amines, and Alkanes <i>via</i> Reduction	6.1 Aldehyde Synthesis by Metal-Free Reduction
6.2	Aldehyde Synthesis by Metal-Mediated Reduction	
6.3	Alcohol Synthesis by Metal-Mediated Reduction	
6.4	Amine Synthesis	
6.5	Alkane Synthesis by Metal-Free Reduction	
7	Making Acid Chlorides from Silyl Esters	
8	<i>In Situ</i> Generated Silyl Esters and Ramifications for Catalysis	
9	Conclusion	

**Key words** silyl ester, carboxylic acid, organosilanes, amidation, reduction

## 1. Introduction

Carboxylic acid derivatives, like esters, amides, and acid chlorides, comprise a diverse class of functional groups that have varying reactivity. The synthesis and/or elaboration of these derivatives represent some of the most common transformations in synthetic chemistry. Carboxylic acid derivatives appear in many synthetic value-added products such as drugs and materials; they can also serve as intermediates to provide enhanced reactivity or protection of the carboxylic acid, allowing access to new molecules.

One such carboxylic acid derivative with unique reactivity and versatility is the silyl ester, where a silicon atom is bonded to at least one acyloxy group.<sup>1</sup> Silyl esters are most commonly discussed as protecting groups of carboxyl functionalities,<sup>2</sup> and are used in this capacity to current day.<sup>3,4</sup> The silylated carboxyl group can be readily deprotected in aqueous media by mild acidic or basic hydrolysis.<sup>2</sup> The stability and reactivity of silyl esters is highly dependent on the steric and electronic properties of the substituents attached to the silicon.<sup>2,5-9</sup> Their labile and adjustable nature lends use in other applications: poly(silyl esters) are well-characterized materials as degradable polymers.<sup>6-8</sup> These polymers are susceptible to decomposition through hydrolysis, but are easily tuned as the stability of the silyl ester depends on the substituents on silicon.<sup>6,8</sup>

Nucleophiles can react with silyl esters (Figure 1) either by attack at the carbonyl group (path I) or by attack at the silicon (path II).<sup>5</sup> As the steric bulk<sup>2</sup> and electron-donating capability of the substituents on silicon increase, so does the hydrolytic stability via path II;<sup>5</sup> this consequently increases the likelihood of nucleophilic attack at the carbonyl group rather than the silicon.<sup>5,6,8,9,10,11</sup> In general, silyl esters are more reactive than alkyl esters with respect to both pathways and this increased reactivity offers opportunities for reaction development.

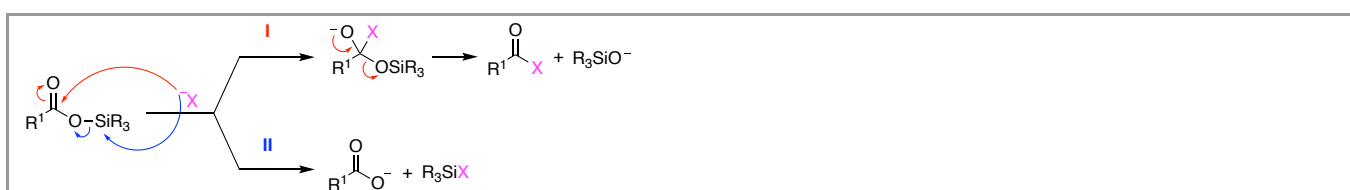


Figure 1 Reaction of silyl esters with nucleophiles.

Silyl esters have increasingly been recognized as powerful reaction intermediates as evidenced by the number of publications in each decade from the 1950s to 2020 that mention silyl esters (Figure 2). The *in situ* formation of silyl esters by the use of organosilicon reagents has been of interest to access these intermediates for further functionalization, such as amidation, esterification, and aldehyde/alcohol synthesis. Organosilicon compounds are highly attractive reagents in organic synthesis due to their availability, ease of use, and environmentally benign nature.

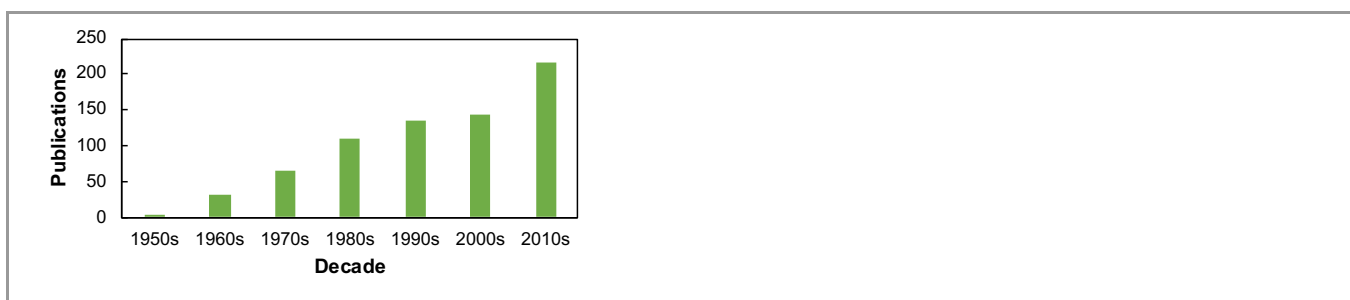
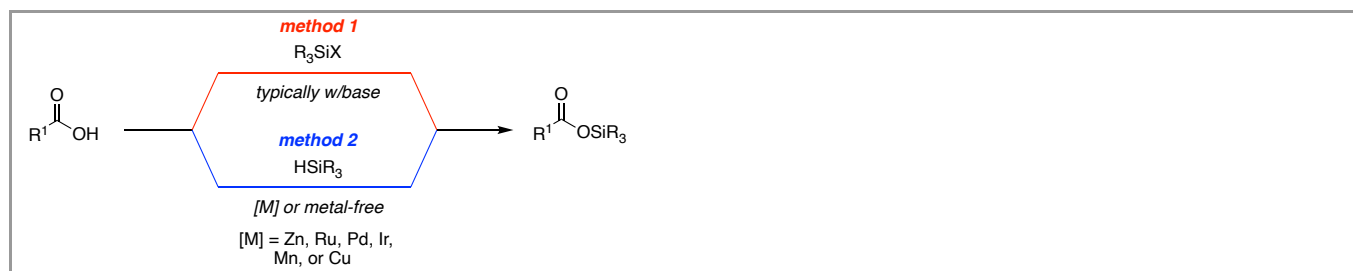


Figure 2 Number of publications per decade from 1950-2020 that mention a silyl ester.

This review aims to provide a comprehensive study of silyl esters as a reactive intermediate. In many cases silyl ester generation is intentional, but we also present case studies to show that silyl esters are generated unintentionally in many catalytic reactions that employ silanes as terminal reductants. The mechanisms of some of these reactions are also considered and their ramifications can offer important insights that can aid in the design of improved silicon-mediated transformations. We have assembled this review to draw attention to silyl esters as powerful, and in many cases, overlooked reactive intermediates in organic synthesis, which we hope will enable future research in this ripe field.

## 2. Synthesis of Silyl Esters

Silyl esters are usually constructed in one of three ways:<sup>12</sup> 1) substitution-type reactions with carboxylate nucleophiles and silane electrophiles (e.g. chlorosilanes<sup>1,2</sup> or aminosilanes<sup>13-15</sup>) (Figure 3, in red), 2) dehydrogenative cross-coupling of carboxylic acids and silanes<sup>16-23</sup> (Figure 3, in blue), or 3) reduction of CO<sub>2</sub> (Figure 4), which exclusively allows access to silyl formates. The substitution-type reaction is the simplest and most convenient method to make silyl esters, however, the unavoidable formation of HCl when reacting carboxylic acids and chlorosilanes has led to the development of alternative methods. The dehydrogenative cross-coupling is frequently catalyzed by transition metals and metal complexes. Simple metal salts such as ZnCl<sub>2</sub> are known,<sup>18</sup> but these reactions are typically catalyzed by transition metals and metal complexes including Ru, Pd, Ir, Mn, Cu(PPh<sub>3</sub>)<sub>3</sub>Cl, or [Ph<sub>3</sub>PCuH]<sub>6</sub>.<sup>16,17,19-21,23</sup> PPh<sub>3</sub> has also been reported to catalyze the dehydrogenative coupling of carboxylic acids and silanes.<sup>17,22</sup> Dehydrogenative cross-coupling of carboxylic acids and silanes has also been observed in the presence of an amine to obtain the silyl ester.<sup>24-26</sup>



**Figure 3** General methods for the synthesis of silyl esters.

Finally,  $CO_2$  can be converted into a silyl formate upon the reaction with a hydrosilane, typically in the presence of a metal catalyst<sup>27</sup>, and this reactive intermediate can be further functionalized into useful products (Figure 4). This method represents a large class of synthetic routes for silyl ester formation and there are numerous reaction protocols that allow for the hydrosilylation of  $CO_2$ . The silyl formate intermediates can be converted to a number of useful molecules such as formamides, silyl acetals, methoxysilanes, methanol, methane, formic acid, *N*-methylamines, formaldehyde<sup>28</sup>, and heterocycles<sup>29</sup> (Figure 4).<sup>30–33</sup> These transformations, however, are somewhat limited in their impact to synthetic organic chemistry as silyl formates provide only a C1 building block for synthesis. There are a vast number of synthetic methods that use hydrosilanes to reduce and then further convert  $CO_2$ ; in some cases, the silyl ester intermediate is explicitly discussed<sup>34–39</sup> and in others it is not.<sup>40,41</sup> Because 1) there are a large number of reactions in this class, 2) generally the role of the silyl formate in these overall transformation is not discussed in detail, and 3) there were recent reviews published on hydrosilylation of  $CO_2$ ,<sup>31,32</sup> we will only cover this class of reactions cursorily in this review.

### 3. Making Amides from Silyl Esters

Amides are regarded as one of the most important functional groups in all areas of organic chemistry and the relevance of amides calls for innovation to develop methods that are practical, efficient, and green.<sup>42</sup> Interest and exploration in the field of silane-mediated coupling for the synthesis of amides have increased over the past decade.<sup>43</sup> Highly efficient, operationally simple, and greener methods for direct amidation using silicon-based coupling reagents have been developed and have also been used to make amide intermediates.

Coupling reagents are used in amide synthesis in order to provide kinetic activation of the acid and ensure the generation of thermodynamically favourable products. The most widely used coupling reagents are carbodiimides (e.g. DCC), uronium salts (e.g. HBTU), phosphonium salts (e.g. BOP), and 1-hydroxy-1*H*-benzotriazole. Despite obtaining high yields, they result in poor atom economy, and are costly and hazardous.<sup>44–46</sup> Catalytic methods, such as those using boronic acids<sup>47–51</sup> or boronic acid esters,<sup>52,53</sup> are used to improve atom economy and limit waste.<sup>54</sup> However, these protocols require hazardous solvents such as dichloromethane and desiccants such as molecular sieves. Overall, while catalytic methods are available and continuously being explored<sup>55</sup> there is still a definitive need for atom-economical stoichiometric reagents. Silicon-based stoichiometric coupling reagents (Figure 5) offer an alternative and, in many cases, atom economical approach to amide synthesis through the intermediacy of silyl esters and path II (Figure 1).

The silanes that we review have been used as coupling reagents for direct amide bond formation and exhibit varying reactivity, but all activate the carboxylic acid to allow for amidation. Chlorosilanes work efficiently in amide and peptide coupling to generate the silyl ester, but the inevitable formation of HCl pose a risk to chiral centers. Aminosilanes work well owing to the stronger Si-O bond allowing for silylation of the carboxylic acid; however, the hydrolytic stability of the starting aminosilanes can hamper their ultimate utility. Alkoxysilanes readily form the silyl ester due to the labile alkoxy groups with silica as one of the only by-products. Hydrosilanes, more specifically arylsilanes, effectively form silyl esters by loss of  $H_2$  allowing for amidation. Commercially available silanes are used, and simple by-products are reported. Overall, the use of silicon-based coupling reagents provides a mild and efficient alternative to common stoichiometric coupling reagents for amide synthesis, where the carboxylic acid is activated *in situ* to a silyl ester.

#### 3.1 Amidation using Chlorosilanes

Early studies on organosilane-mediated amide coupling reactions involved the investigation of silicon tetrachloride ( $SiCl_4$ ). In 1969, Chan and Wong first reported the use of  $SiCl_4$  for amide coupling in pyridine (Figure 6).<sup>56</sup> In 1971, the same researchers extended the use of this reagent as a coupling reagent for peptide synthesis.<sup>57</sup> They proposed that they could initially react the *N*-protected amino acid with  $SiCl_4$  to form a tetraacyloxysilane **1** (Figure 7). Subsequent reaction of the acyloxysilane (**1**) with the unprotected amine of the amino ester can then yield the amide through nucleophilic attack at the carbonyl. They achieved efficient peptide synthesis; however, extensive racemization was observed after the formation of the dipeptide.

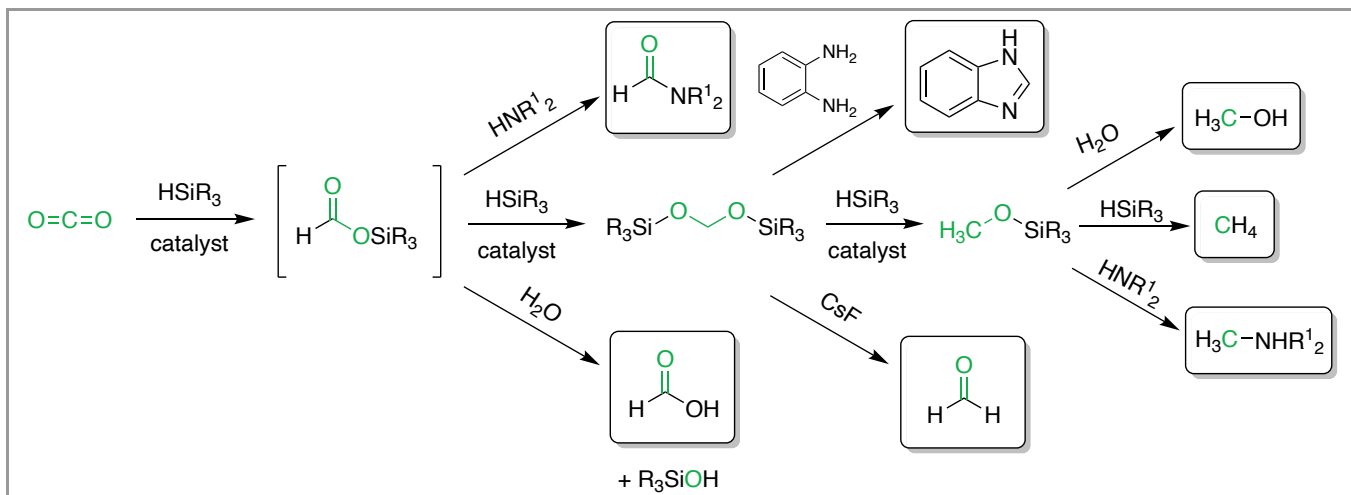


Figure 4 Hydrosilylation of CO<sub>2</sub> into a silyl formate and examples of subsequent functionalization.

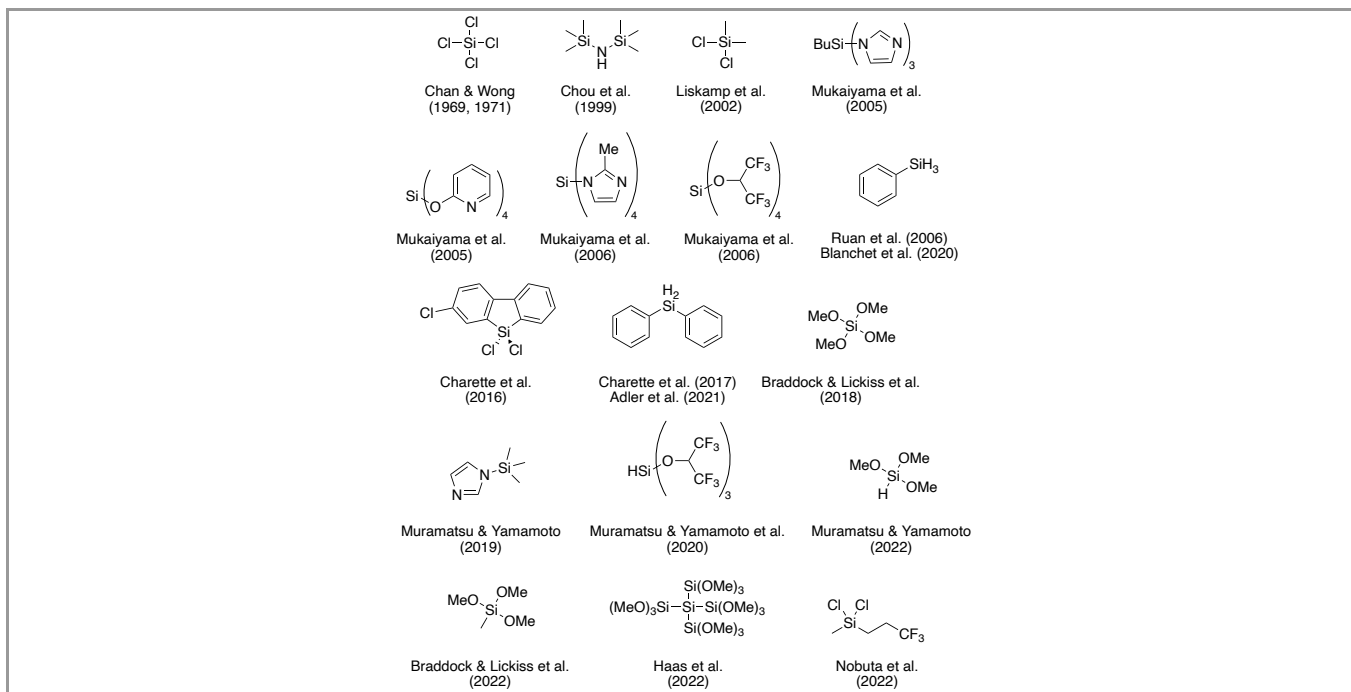


Figure 5 Silicon coupling reagents used in amidation and peptide coupling.

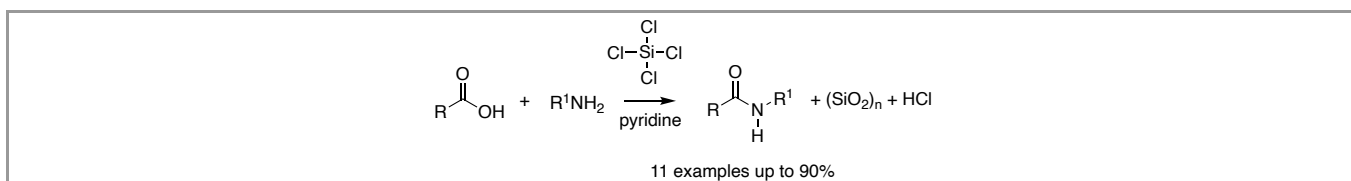


Figure 6 SiCl<sub>4</sub>-mediated amide coupling.

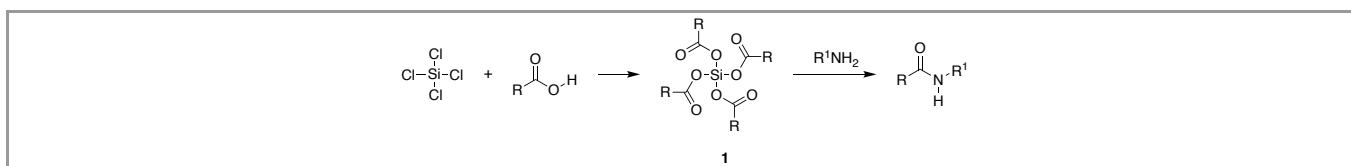


Figure 7 Initial formation of tetraacyloxysilane **1**, followed by nucleophilic attack of the amine to form the amide.

Dichloroalkylsilanes were investigated by Liskamp and co-workers for the synthesis of dipeptides using a simultaneous *N*-protection and carboxyl-activation strategy.<sup>58</sup> Dichloromethylsilane ( $\text{Me}_2\text{SiCl}_2$ ) was reacted with *L*-phenylalanine in pyridine, which acted as an acid scavenger. This was then reacted with an amine to form the corresponding amide in quantitative yield (Figure 8). Sterically hindered amines performed poorly in this reaction. Primary amines attached to a methylene gave excellent yields, while branched primary amines had lower yields. Mechanistic investigations showed that the reaction requires an unprotected  $\alpha$ -amine on the carboxylic acid coupling partner, suggesting that a cyclic species **2**, an oxazasilolidinone, is the reactive intermediate (Figure 8). A silyl ester intermediate initially forms from the carboxylic acid and  $\text{Me}_2\text{SiCl}_2$ , and cyclization occurs from nucleophilic attack of the free amine at the carbonyl carbon to give **2**.  $^1\text{H}$  NMR experiments also supported the presence of the cyclic intermediate, though attempts to isolate the cyclic intermediate were unsuccessful. The authors investigated the regiochemistry of the method when two carboxylic acid functionalities are present in the amino acid. For the dichlorodimethylsilane-mediated amidation of *L*-aspartic acid, the use of pyridine as the base/solvent resulted in an equimolar ratio of the two regioisomeric products. However, high selectivity for the  $\alpha$ -product was observed when triethylamine (TEA) was used as the base/solvent (Figure 9). With pyridine, the thermodynamically favoured six-membered cyclic intermediate **3'** is formed; the authors proposed that TEA, as the stronger base, provided the kinetically favoured five-membered cyclic intermediate (**3**) preferentially.

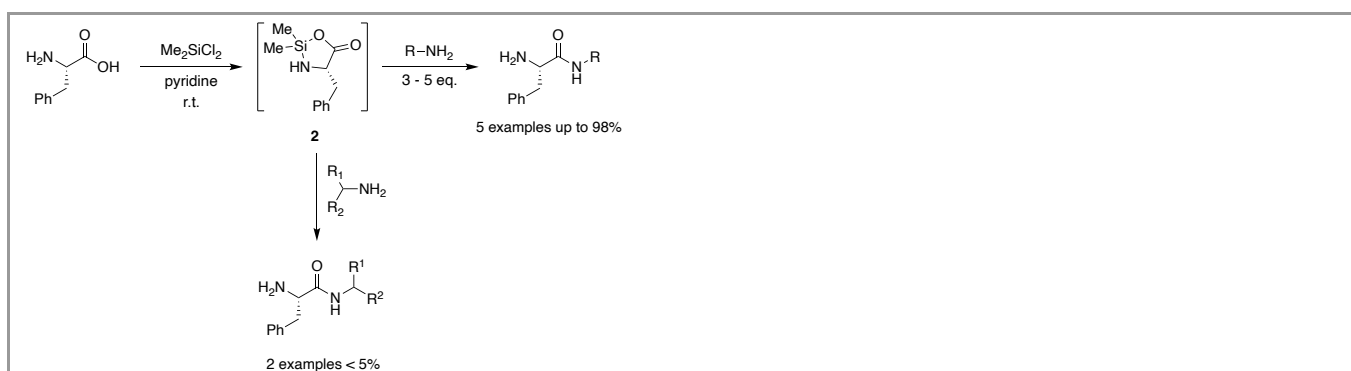


Figure 8 Dichlorodimethylsilane-mediated amide synthesis.

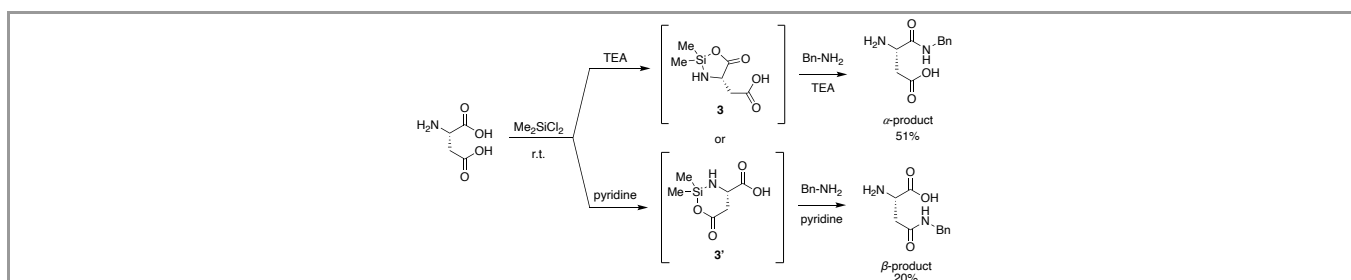


Figure 9 Regioselectivity of dichlorodimethylsilane-mediated amide coupling.

In a similar strategy to Liskamp *et al.*'s method, Nobuta and co-workers explored dichloro(methyl)(3,3,3-trifluoropropyl)silane (MTFPSCl<sub>2</sub>) as a coupling reagent in the amidation of various unprotected amino acids using  $\alpha$ -branched amines and anilines (Figure 10).<sup>59</sup> They propose oxazasilolidinone intermediate **4** to simultaneously activate the carboxylic acid and protect the free amine on the amino acid residue (Figure 10). The authors hypothesized that the electron-withdrawing fluorinated alkyl group on the silicon will increase the electrophilicity of the silicon allowing enhanced reactivity with more sterically challenging nucleophiles, which was an issue reported using  $\text{Me}_2\text{SiCl}_2$  in Liskamp and co-workers' method.<sup>58</sup> Mechanistic investigations showed that the nucleophilic amine at the  $\alpha$  position on the unprotected amino acid residue is necessary for amidation using MTFPSCl<sub>2</sub>.<sup>59</sup>

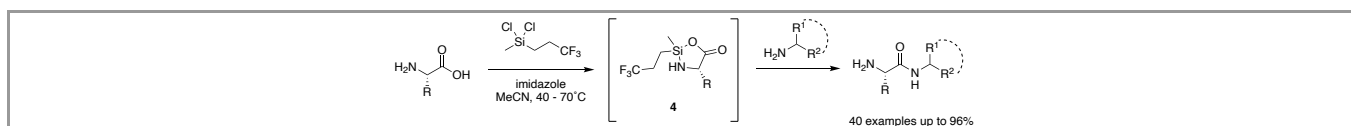


Figure 10 Proposed intermediate **4**, and subsequent amide formation.

In 2016, the Charette group synthesized and investigated novel 9-silafluorenyl dichlorides (Figure 11) as coupling reagents for peptide synthesis from unactivated amino esters and *N*-protected amino acids.<sup>60</sup> A simple amide coupling reaction of glycine methyl ester hydrochloride salt and phenylacetic acid with various commercially available chlorosilanes showed that this reaction can proceed in good yield using diphenyldichlorosilane along with,  $\text{Et}_3\text{N}$  and DMAP. In reactions using more sterically hindered amino acid residues the yield significantly decreased. They proposed that the bulky nature of the silane and amino acids were hindering the approach of the residues

around the silicon. They then modified the silane coupling reagent to exploit the flatness and rigidity of 9-silafluorenyl dichloride (**5**), which has similar electronic properties to diphenyldichlorosilane. Again, using glycine methyl ester hydrochloride salt and phenylacetic acid, the amide product was synthesized in good yield using **5**. Small molecule amides were obtained with **5** in good to excellent yields and no epimerization of stereocenters was observed. Dipeptide synthesis was attempted, and reaction yields were good but needed improvement to compete with existing methods of peptide coupling.

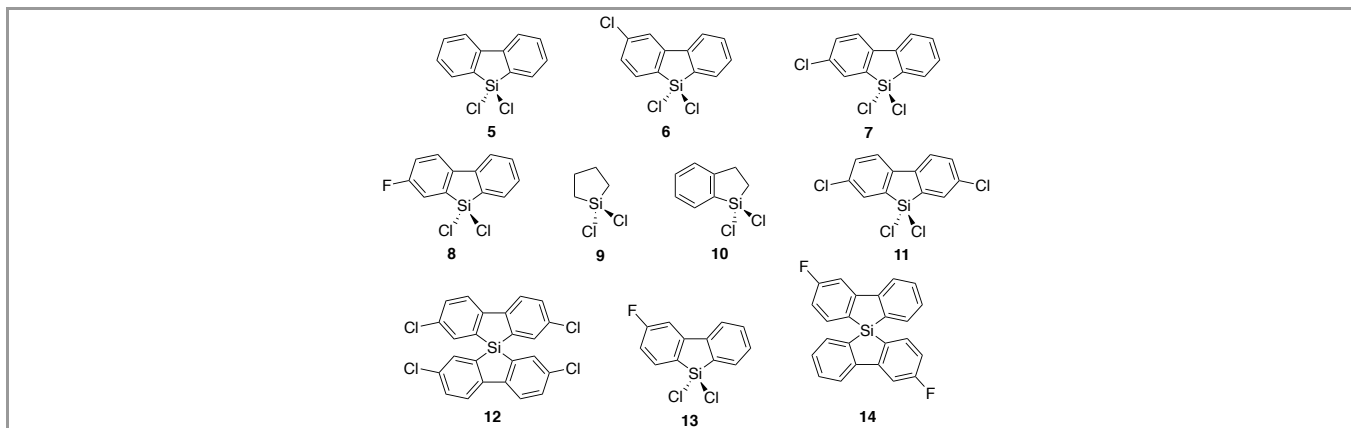


Figure 11 Synthesized dichlorosilane by Charette *et al.*

The 9-silafluorenyl dichloride **5** was further modified to add electron-withdrawing substituents to make it more electrophilic. The formation of the sterically challenging Boc-L-Phe-L-Phe-OMe dipeptide revealed higher reaction yield with the halo-substituted 9-silafluorenyl dichlorides (**6-8**) when compared to unsubstituted 9-silafluorenyl dichloride. **7** gave the highest yield, and the authors suggest it has the optimal steric and electronic properties for this reaction. Furthermore, it was used in a series of peptide reactions (Figure 12) and various peptides were synthesized in good to excellent yields. Tripeptides were also made in good yields. A dipeptide was used to investigate epimerization and enantiospecificity was found to be 86%.

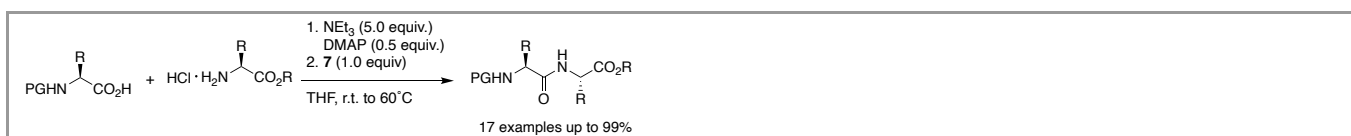


Figure 12 Optimized peptide coupling reactions.

### 3.2 Amidation using Azasilanes

Chou *et al.* synthesized various *N*-acylalkylenediamines by the monoamidation of unactivated carboxylic acids with diamines in the presence of HMDS for the application of making hypertensive drugs (Figure 13).<sup>61</sup> They report that amines are not readily silylated by HMDS, so amidations occur selectively in high yields. The reaction (Figure 13) worked well with aliphatic and aromatic carboxylic acids as well as with acyclic and cyclic diamines. The authors also demonstrated that HMDS promotes monoamidation of the carboxylic acid when using acyclic and cyclic diamines. This was proved as they treated the monoamide product with more acid and HMDS, and no diamide was observed despite the presence of the free secondary amine.

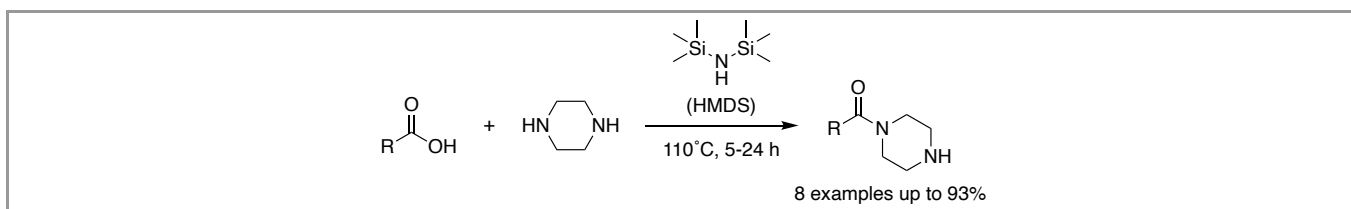


Figure 13 HMDS-mediated amide bond formation.

Between 2005 and 2006, Mukaiyama and co-workers investigated various organosilane reagents as dehydrating reagents in the condensation of carboxylic acids and amines.<sup>62-65</sup> They described two methods using imidazol-1-ylsilane derivatives (Figure 14, **15** and **16**) that produce amides via formation of a 1-acylimidazole intermediate **18** (Figure 15).<sup>62,65</sup> The authors speculated that the reaction proceeds through the silyl ester intermediate **17**, which subsequently forms the 1-acylimidazole (**18**) by nucleophilic attack of the liberated imidazole (Figure 15). Several carboxylic acids and amines were reacted in the presence of **15** or **16** giving different amides in good to excellent yields.

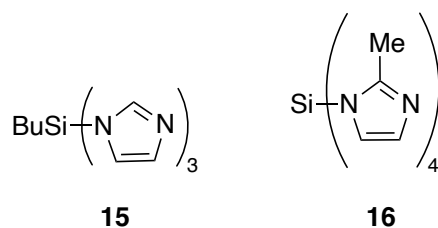


Figure 14 Coupling reagents used by Mukaiyama and co-workers.

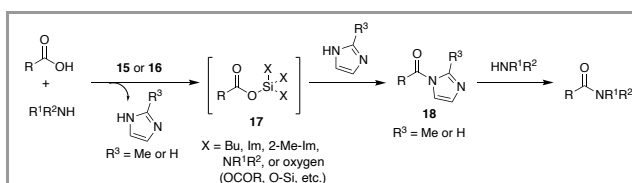


Figure 15 Amidation using **15** and **16**.

Muramatsu, Yamamoto, and co-workers also investigated imidazolyl silanes for amide bond formation.<sup>10a</sup> They developed peptide coupling methods using  $\text{Ta}(\text{OMe})_5$  and 1-(trimethylsilyl)imidazole (**19**) (Figure 16). They found that  $\text{Ta}(\text{OMe})_5$  was the optimal Lewis acid with **19** to activate the carbonyl group of the silyl ester (**20**) that is formed *in situ* (Figure 17).<sup>10a</sup> They synthesized various peptides using amino acids and amino esters with different protecting groups and functional groups, without any epimerization. The liberated imidazole (after silylation of the amino acid) was crucial for the neutralization of HCl when using the HCl salt of different amino esters. They also extended their method to chemoselective amidation with an ester present on the carboxylic acid, amidation of  $\gamma$ - to  $\lambda$ -homoamino acids, and small molecule amides.

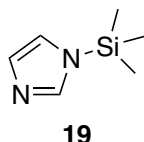


Figure 16 Azasilane used by Muramatsu and Yamamoto.

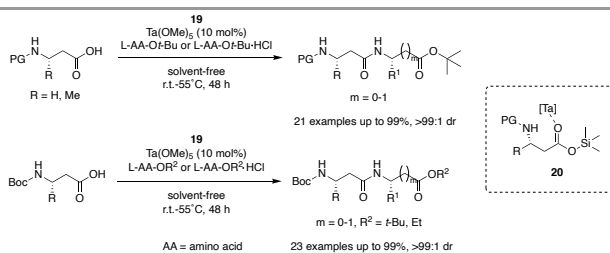


Figure 17 Scope of **19**-mediated peptide coupling.

### 3.3 Amidation using Oxysilanes

Mukaiyama and co-workers also explored alkoxy silanes for the condensation of carboxylic acids and amines (Figure 18). They used **21** (tetrakis(pyridine-2-yloxy)silane) as a novel dehydrating reagent.<sup>63</sup> The proposed reaction mechanism using **21** (Figure 19) shows that first the carboxylic acid reacts with **21** to form a silyl ester intermediate (**23**), with the elimination of 2-hydroxypyridine (2-PyOH). When using **15** or **16**, the active species is 1-acylimidazole,<sup>62</sup> but here 2-hydroxypyridine is weakly nucleophilic and no other active intermediates are observed. They speculate that the reactive silyl ester intermediate directly undergoes condensation with amines to afford the amides.

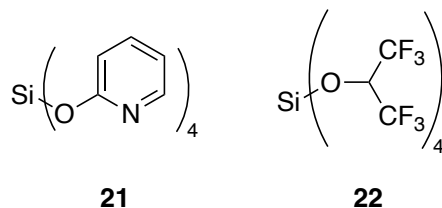


Figure 18 Coupling reagents used by Mukaiyama and co-workers.

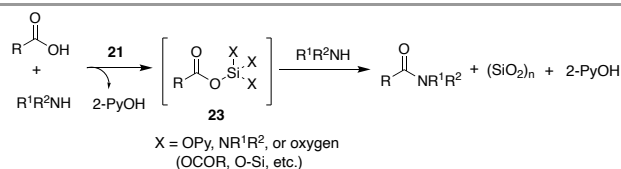


Figure 19 Amidation using **21**.

Mukaiyama and co-workers further found that tetrakis(perfluoroalkoxy)silanes, such as **22**, enabled the condensation reaction of a carboxylic acid and an amine.<sup>64</sup> They observed that tetrasubstituted silanes having fluoro-substituted alkoxy groups showed improved reactivity, with **22** being the most effective. The authors considered that **22** reacts with a carboxylate to form silyl ester intermediates (**25**) (Figure 20). More sterically hindered carboxylic acids resulted in two products: the amide or perfluoroalkyl esters. This is due to the competing nucleophilic attacks of the amine and the liberated perfluorinated alcohol toward the silyl ester intermediate. **22** gave several amide products in high yield without the undesirable side-products due to low nucleophilicity of the perfluorinated alcohol **24**.

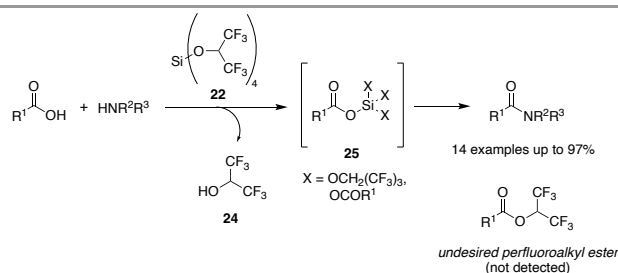


Figure 20 Reaction pathway of **22**-mediated amide synthesis.

Braddock and Lickiss *et al.* investigated the use of tetraalkyl orthosilicates as amide-coupling reagents.<sup>66</sup> They found efficient direct amidation reaction conditions using commercially available, tetramethylorthosilicate (TMOS) (Figure 21). Their method was applicable to aliphatic and aromatic carboxylic acids and amines with varying functional groups, and the only by-product was silica. TMOS was also an effective coupling reagent in the synthesis of Moclobemide and nitrobenzenamide, a precursor to an antiarrhythmic drug, and other sterically challenging substrates. The amides were synthesized without the need for any chromatographic purification; however, the reaction requires a 200 mol % loading of tetramethylorthosilicate, which is also quite toxic. The authors postulated a silyl ester intermediate **26** as the most likely acylating agent (Figure 22). When benzoic acid was mixed with TMOS in refluxing toluene for 1 h, they observed **26** by <sup>1</sup>H, <sup>13</sup>C, and <sup>29</sup>Si NMR spectroscopy. Even in the presence of benzylamine, the silyl ester was observed.

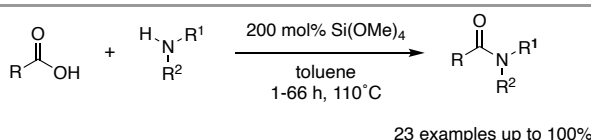


Figure 21 TMOS as a coupling reagent in direct amide bond formation.

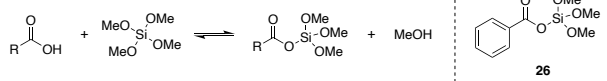
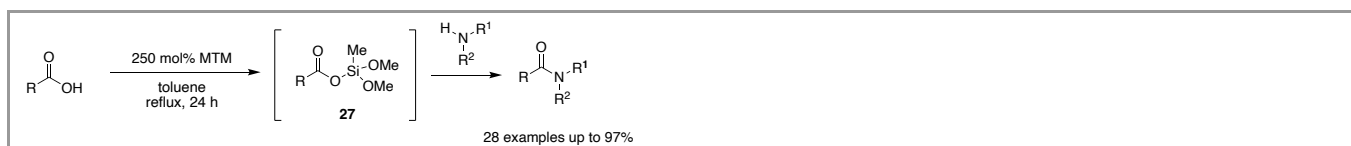


Figure 22 Formation of silyl ester intermediate **26**.

TMOS readily hydrolyzes to silica and is considered fatal if inhaled, making it toxic to work with and an unappealing coupling reagent to use. In their subsequent work, Braddock and Lickiss use methyltrimethoxysilane (MTM) as a coupling reagent in direct



amidation as it has similar reactivity to TMOS, but does not hydrolyze to silica, making it a safer alternative. Various amides were synthesized using MTM and isolated without the requirement of chromatography.<sup>67</sup> Mechanistically, silyl ester **27** is proposed to form followed by nucleophilic attack of the amine to form the amide product (Figure 23).<sup>67</sup>



**Figure 23** Amide formation using MTM and proposed silyl ester intermediate **27**.

Recently, Haas and co-workers investigated the use of polysilanes, hexamethoxydisilane **28** and dodecamethoxyneopentasilane **29** for amide bond formation and were able to synthesize different amides with low coupling reagent loading (Figure 24).<sup>68</sup> They took advantage of the lower bond energy of Si-Si bonds compared to Si-O bonds, which would make the silane more reactive in the formation of silyl ester intermediates in comparison to TMOS. Each silicon in **28** and **29** acts as a reactive site for the formation of the silyl ester by reaction with the carboxylic acid.<sup>68</sup>

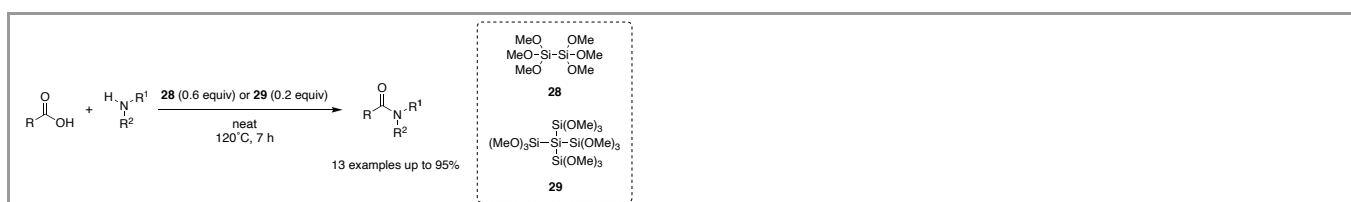


**Figure 24** Amide formation using methoxysilanes.

Muramatsu, Yamamoto, and co-workers were also interested in silane-mediated amide bond formation using alkoxy silanes. They developed coupling methods using  $\text{HSi}(\text{OCH}(\text{CF}_3)_2)_3$  (**30**) and an aminosilane catalyst (Figure 25).<sup>69</sup> They also reported the use of trimethoxysilane (**31**) with **30** as a catalyst (Figure 25).<sup>70</sup>

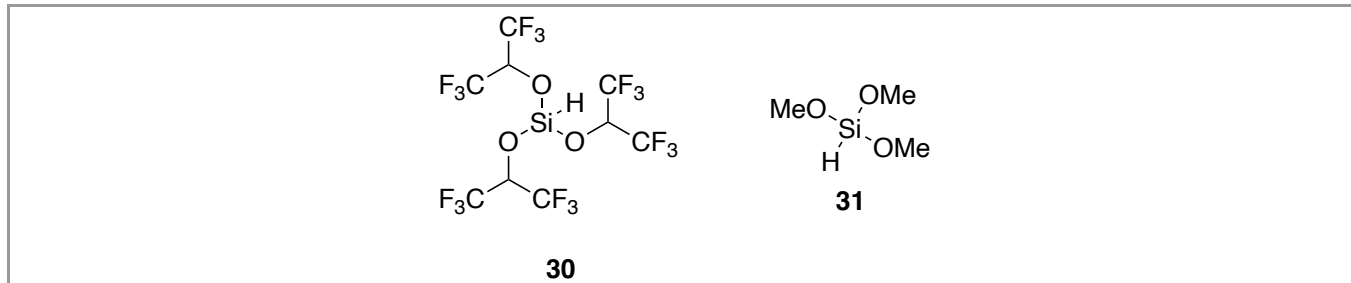


**Figure 25** Alkoxy silanes used by Muramatsu and Yamamoto.

Muramatsu, Yamamoto, and co-workers reported a **30**-mediated peptide coupling reaction and the use of an aminosilane catalyst to accelerate amide synthesis.<sup>69</sup> Of the investigated silanes,  $\text{HSi}(\text{OCH}(\text{CF}_3)_2)_3$  (**30**) worked the best to give the peptide with no epimerization. Dipeptides were synthesized in good to excellent yields and high diastereomeric ratios (Figure 26), and their method showed a wide functional group tolerance and applicability to several amino acids.

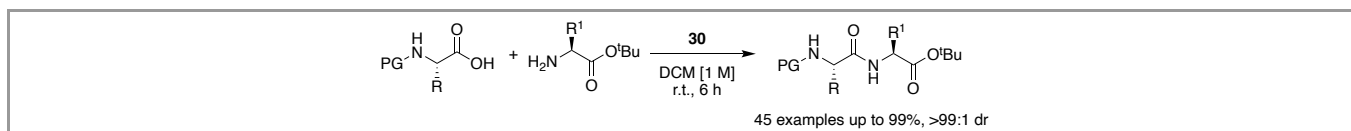
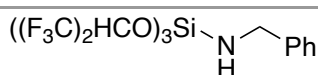


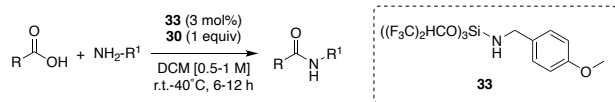
**Figure 26** Scope of reaction using **30** (in all cases R or R<sup>1</sup> = Me).

During mechanistic studies they found that the addition of an aminosilane **32** (Figure 27) significantly accelerated the formation of proposed silyl ester intermediates. The authors speculate that the aminosilane may play a role as a Lewis acid to increase the acidity of the carboxylic acid groups. A series of aminosilane catalysts were explored and they found that 3 mol% of **33** with **30** improved the yields for a variety of peptides without compromising diastereomeric ratios (Figure 28). A precursor of nonsteroidal anti-inflammatory drug (NSAID)-glucosamine bioconjugates were synthesized, and this method was also useful for the synthesis of small molecule amides.



**32**

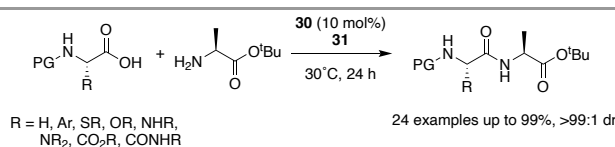
**Figure 27** Aminosilane found to accelerate silyl ester formation.



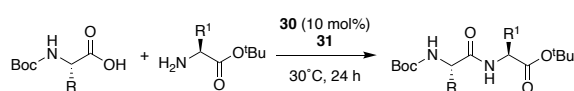
24 examples up to 99%, >99:1 dr

**Figure 28** Scope of reaction using **33** as a catalyst with silane **30**.

Recently, Muramatsu and Yamamoto expanded on their method using **30**, and report a catalytic approach where **30** is used to activate **31**. Trimethoxysilane **31** was found to be the optimal silane for peptide formation. A wide variety of *N*-protected amino acids bearing a variety of functional groups were used in this reaction to synthesize peptides in high yields and high diastereomeric ratios (Figure 29). Further investigating the synthetic utility of their method, many *t*-butyl esters of amino acids and peptides were explored (Figure 29). Many amino esters were tolerated in this reaction with varying functional groups; however, lower yields were obtained with sterically challenging substrates.<sup>70</sup>



24 examples up to 99%, >99:1 dr



20 examples up to 99%, >99:1 dr

**Figure 29** Scope of **31**-mediated peptide formation using **30** as a catalyst.

### 3.4 Amidation using Hydrosilanes

Ruan and co-workers were first to explore commercially available phenylsilane as an amide-coupling reagent and were able to synthesize amides and peptides in excellent yields, both in solution and solid-phase (Figure 30).<sup>71</sup> Minimal racemization was observed when used for peptide synthesis.

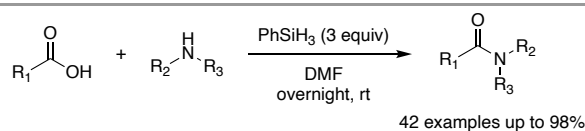


**Figure 30** Phenylsilane as a coupling reagent as reported by Ruan *et al.*

In 2020, Blanchet and co-workers further investigated phenylsilane as a coupling reagent for the synthesis of small-molecule amides, peptides, and Weinreb amides.<sup>25</sup> Optimization studies done in acetonitrile found that an excess of carboxylic acid and phenylsilane were needed to obtain high yields of the amides. Various carboxylic acids were coupled to primary and cyclic secondary amines in good to excellent yields (Figure 31).

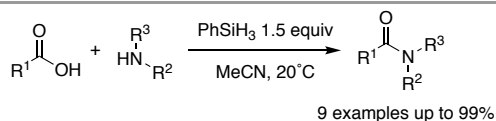


**Figure 31** Phenylsilane-mediated amidation proposed by Blanchet *et al.*

Phenylsilane was also found by Blanchet *et al.* to be effective in peptide couplings and in the synthesis of Weinreb amides. The authors coupled various *N*-protected amino acids and  $\alpha$ -amino esters in moderate to good yields (Figure 32a). Protecting groups on these substrates were generally well tolerated and no epimerization was detected. Tripeptides, however, were only synthesized in moderate yields. To make Weinreb amides, the hydrochloride salt of *N,O*-dimethylhydroxylamine was reacted with various aliphatic and electron

deficient aromatic carboxylic acids (Figure 32b); these reactions proceeded in moderate to good yields. After mechanistic investigations suggested that a triacyloxysilane is the reactive intermediate, the authors explored silicon tetraacetate (**34**) as a general acetylating agent of amines, and various acetamides were synthesized in good to excellent yields (Figure 32c).

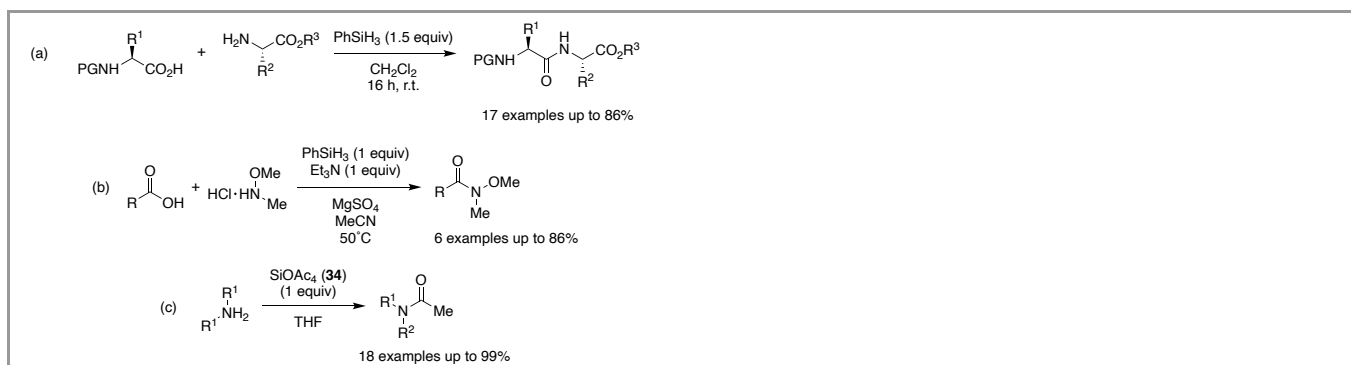


**Figure 32** (a) Peptide coupling using phenylsilane. (b) Weinreb amide synthesis. (c) Synthesis of acetamides.

In 2012, Ashfeld and co-workers reported a catalytic Staudinger ligation reaction using a free carboxylic acid, azide, phenylsilane, and catalytic triphenylphosphine (Figure 33).<sup>72</sup> Various amides and dipeptides were synthesized in good to excellent yields using this method. They did not propose the formation of a silyl ester intermediate, however, Andrews and Denton,<sup>73</sup> and later White and Mecinović *et al.*<sup>74</sup> describe a mechanism showing the formation of a reactive silyl ester as discussed in Section 8.

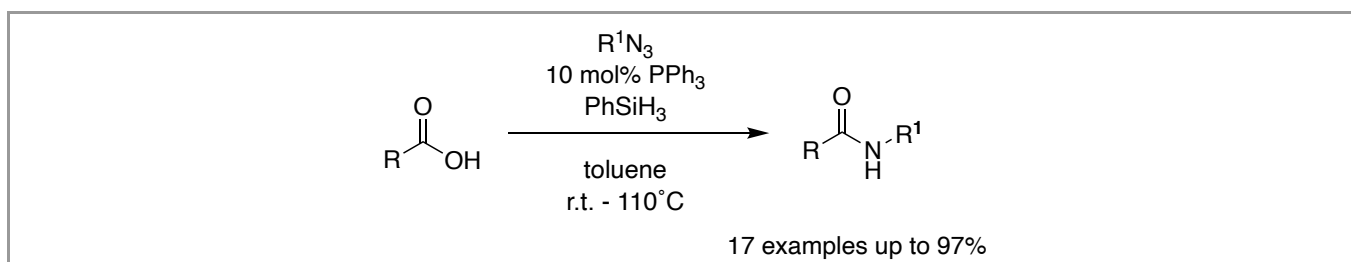


**Figure 33** Phosphine-catalyzed Staudinger ligation.

Aside from phenylsilane, other commercially available hydrosilanes, such as diphenylsilane has also shown to be effective in amidation. Charette *et al.* were also interested in commercially available diphenylsilane as a coupling reagent and developed a direct amidation reaction of unactivated carboxylic acids and amines using diphenylsilane.<sup>26</sup> They optimized reaction conditions and expanded their substrate scope to various carboxylic acids and amines in excellent yields (Figure 34). Their method also worked well in the synthesis of peptides upon the addition of a base and additive (Figure 35).

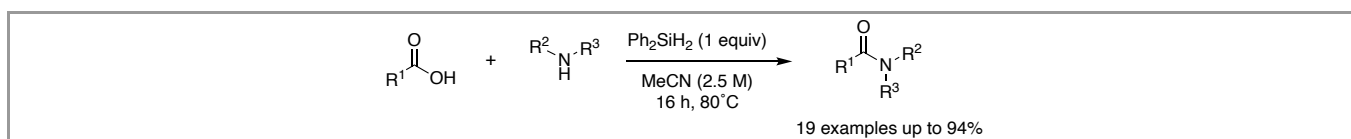


**Figure 34** Diphenylsilane-mediated amide coupling reaction by Sayes and Charette.

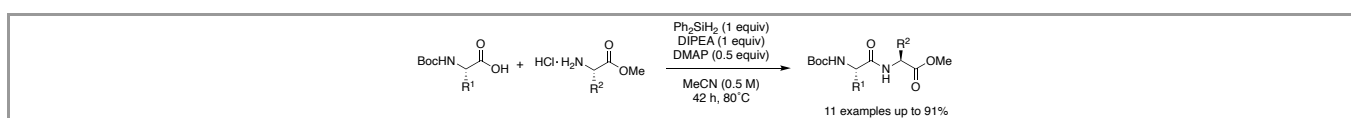


**Figure 35** Diphenylsilane-mediated peptide and lactam coupling by Sayes and Charette.

Recently, the Adler group has further investigated the use of diphenylsilane as an amide-coupling reagent.<sup>75</sup> They found efficient direct amidation reaction conditions using diphenylsilane and the addition of a tertiary amine base, *N*-methylpyrrolidine; this additive presumed to enhance the reaction by deprotonating the carboxylic acid to make a more soluble ammonium carboxylate salt and maintain the nucleophilicity of the amine substrate. Amidation was optimal without rigorous exclusion of air or water, and various amides were synthesized in good to excellent yields, with good functional group tolerance by thermal heating, microwave heating, or at room temperature (Figure 36).

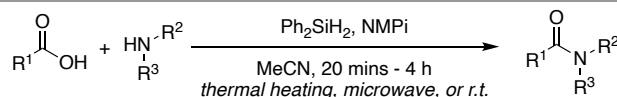


**Figure 36** Diphenylsilane-mediated amide coupling reaction with a tertiary amide additive by Adler *et al.*

### 3.5 Amine Formation *via* Amidation/Reduction

Amines can be made indirectly from the silyl ester *via* reduction of amides made using silanes. This work demonstrates how an understanding of silyl esters, and their reactivity can be harnessed to develop reactions in which silyl esters play multiple roles. In this case they are intimately involved in the activation of the carboxylic acid and the reduction of the amide intermediates. In 2016, Denton *et al.* developed a method for the catalytic reductive *N*-alkylation of amines using carboxylic acids.<sup>76</sup> Their strategy involved a phenylsilane-mediated C-N bond formation followed by catalytic amide reduction. The authors improved the atom-economy of Ruan's phenylsilane method<sup>71</sup> for amide bond formation by reducing the equivalents of phenylsilane and using refluxing toluene instead of DMF at room temperature. They found that 1 mol% of an iridium catalyst ( $[\text{Ir}(\text{COD})\text{Cl}]_2$ ) with additional equivalents of phenylsilane provided the amine product.<sup>77</sup>

Many tertiary amines were obtained in good to excellent yields using various aliphatic and aromatic carboxylic acids (Figure 37a). More hindered aliphatic carboxylic acids were tolerated, however, sterically hindered amines led to lower conversions. Conditions for synthesizing secondary amines from carboxylic acids and primary amines were also established (Figure 37b); this was more challenging due to the decreased Lewis basicity of the secondary amide intermediate. Primary aliphatic acid and sterically hindered carboxylic acids and amines were efficient in the synthesis of secondary amines. While many functional groups were tolerated, phenols were silylated and reducible functional groups (such as alkenes, nitriles, nitro groups and esters) were susceptible to competing reduction reactions.

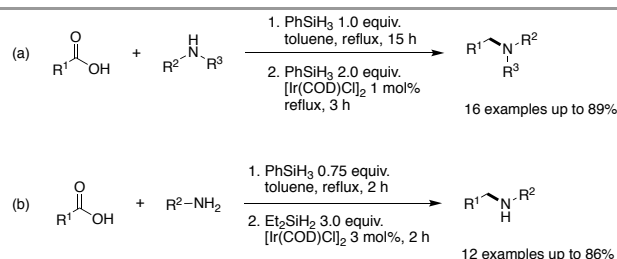


**Figure 37** Synthesis of: (a) tertiary amines, (b) secondary amines.

The authors proposed a tentative mechanism for their reaction that involves an active silyl ester intermediate (Figure 38).<sup>76</sup> Initially, there is base-catalyzed dehydrogenative formation of a silyl ester intermediate **35**, which acts to acylate the amine nucleophile to form the amide. Then in the reduction phase, the Lewis basic amide is activated to **36**; and they speculated this occurs *via* *O*-silylation by a silylated iridium hydride species ( $\text{R}_3\text{Si}-[\text{Ir}]-\text{H}$ ). The reduction of the activated amide **36** could be done by Ir-H as seen in the literature, or the iminium ion may be reduced directly by phenylsilane.

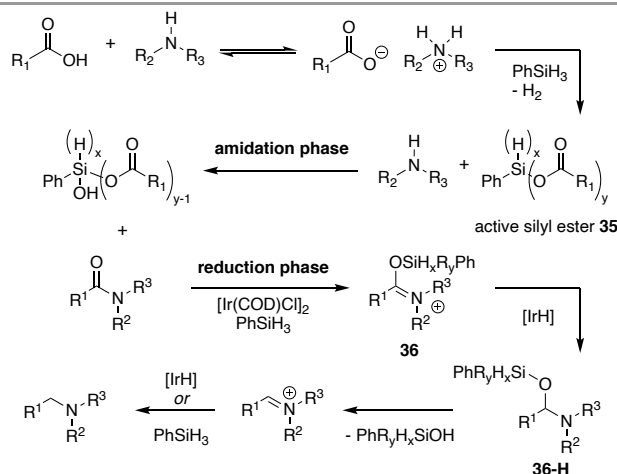


**Figure 38** Mechanism of catalytic reductive *N*-alkylation of amines using carboxylic acids.

Denton and co-workers continued their work with phenylsilane and have used it for silane-mediated amidation followed by  $\text{Zn}(\text{OAc})_2$ -catalyzed amide reduction (Figure 39).<sup>24</sup> These conditions offer advantages over the Ir-catalyzed processes because this allowed for a more general reaction and the use of a simple and inexpensive Zn salt. They found that an excess of carboxylic acid (0.5 equiv.)

resulted in much faster amide reduction (*vide infra*), which allowed both tertiary and secondary amines to be prepared using this method. In the majority of cases the amine products were isolated without chromatography. Their method was also employed for large-scale reductive amination for the synthesis of dibenzylamine, and sequential reductive amination for the synthesis of *N,N*-disubstituted piperazines. The authors were also able to demonstrate selective reduction of a tertiary amide in the presence of a secondary amide, and their method was also used to make Maraviroc, an anti-retroviral medicine.

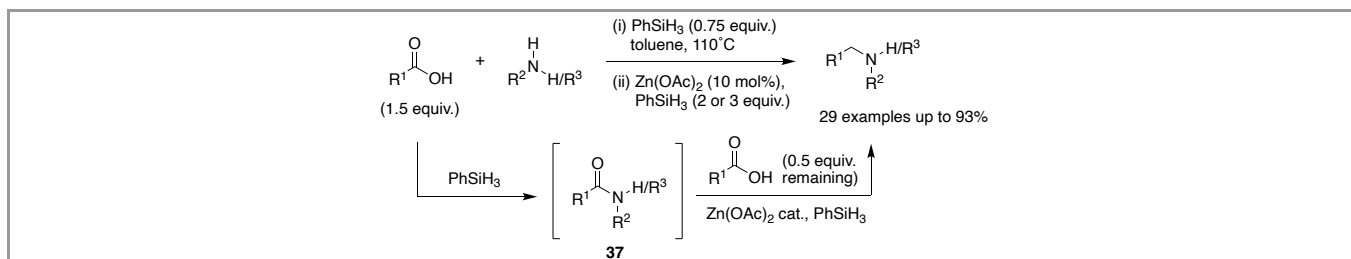


Figure 39 Two phase catalytic reductive amination of carboxylic acids.

Mechanistic investigations were then conducted to understand the role of the carboxylic acid. Their experiments revealed that amide reduction was enhanced in the presence of the carboxylic acid. They speculated that phenylsilane was modified *in situ* by dehydrogenative coupling with the carboxylic acid (Figure 40). This was demonstrated by  $^{19}\text{F}$  NMR spectroscopy using 4-fluorobenzoic acid and a complex mixture of silyl esters were observed. Independent generation of a similar mixture of silyl esters using *N*-methylmorpholine was then carried out and the mixture was shown to reduce a secondary amide. An ester derived from *para*-fluorobenzoic acid was also found to be more reactive than phenylsilane in the presence of  $\text{Zn}(\text{OAc})_2$ .

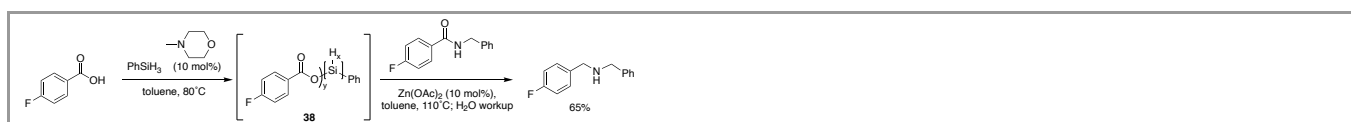


Figure 40 Mechanistic pathway for the formation of **38** and subsequent  $\text{Zn}(\text{OAc})_2$ -catalyzed reduction of an amide.

The authors suggest that the reaction proceeds via phenylsilane-mediated amide synthesis followed by subsequent reduction.<sup>24</sup> First, the carboxylic acid reacts with the phenylsilane to generate a mixture of silyl esters through dehydrogenative silylation. The silyl esters are then activated by  $\text{Zn}(\text{OAc})_2$  to produce the amide, which is followed by activation and reduction of the amide. The mechanism of the final steps (i.e. amide activation and reduction) have not been fully investigated due to the complexity of the silyl esters, but the authors have not ruled out the formation of a zinc hydride and possible exchange of the carboxylic acid for the acetate ligands on zinc. Denton and co-workers also report a method to make trifluoroethylamines from silyl esters, but a different mechanistic pathway is proposed as discussed in Section 6.4.

### 3.6 Miscellaneous

Rostovskaya and co-workers developed a method for synthesizing hydrazides of amino acids and peptides, which proceeded by silylation of the amino acid or peptide (**39**) followed by hydrazinolysis of the trimethylsilyl ester (**40**) (Figure 41).<sup>78</sup> Bis(trimethylsilyl)acetamide (**41**) was used as the silylating agent at room temperature in DMF or methylene chloride, and this afforded the hydrazides of various amino acids and peptides in high yields.

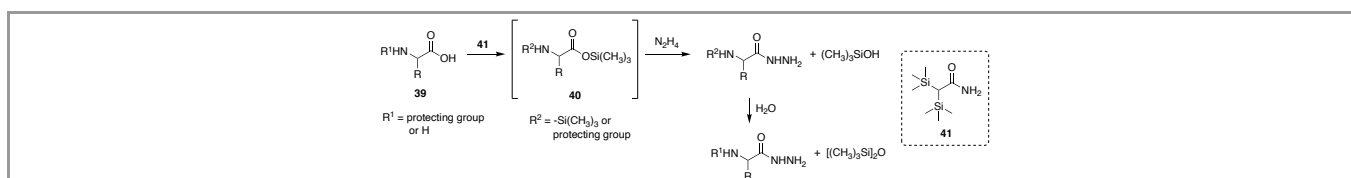


Figure 41 Synthesis of hydrazides.

## 4. Mechanistic Investigations of Amidation

All of the previously discussed amidations in Sections 3.1 to 3.6 rely on the formation of a reactive silyl ester intermediate to activate the carboxylic acid as an electrophile *in situ*. Once the formation of the silyl ester intermediate happens, there are two proposed pathways to make the amide (Figure 42): 1) carboxylic acid activation (in red), in which a nucleophilic amine attacks the carbonyl carbon of the silyl ester, or 2) chemical ligation (in blue), in which the amine first attacks the silicon, and the amide is formed through intramolecular rearrangement and extrusion of a silicon oxide.<sup>26</sup> Although these two pathways are possible, the literature predominantly suggests that silane-mediated amide bond formation generally proceeds through the carboxylic acid activation pathway (in red).

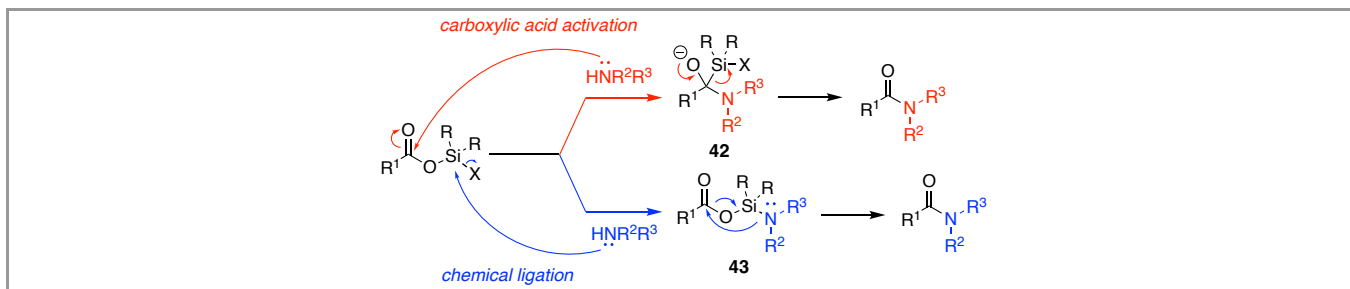


Figure 42 Carboxylic acid activation (in red) vs. chemical ligation (in blue).

#### 4.1 Mechanism of Amidation using Chlorosilanes

Early studies by Chan and Wong using  $\text{SiCl}_4$  as a coupling reagent suggest that their reaction most likely proceeded through intermediate **43** by the chemical ligation pathway (in blue). This pathway was postulated to be the one occurring over carboxylic acid activation (in red) because in a reaction using salicylic acid, only salicylic acid was recovered after hydrolysis. This is because the salicylic acid forms a stable chelate (Figure 43) with silicon and is unable to form **43**, whereas if the carboxylic acid activation pathway was occurring, some product would be obtained due nucleophilic attack at the carbonyl.<sup>56</sup>

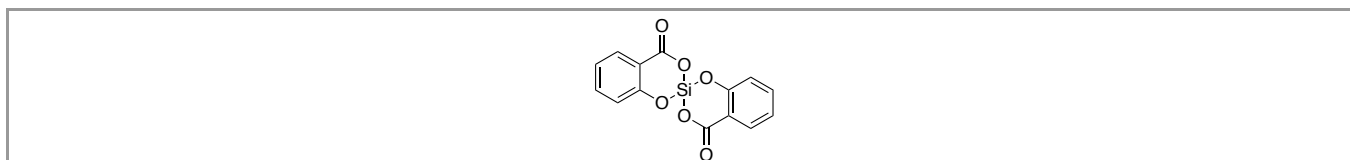


Figure 43 Stable chelate that formed from salicylic acid.

Recent studies in the literature have proposed both pathways, and we will discuss those reports here. Charette and co-workers proposed a chemical ligation pathway (in blue), for their coupling reactions that used 9-silafluorenyl dichloride as a coupling reagent. They noted that with this reagent the amino acids can be tethered together (Figure 44), which can rearrange upon heating to give the amide bond and a siloxane polymer.<sup>60</sup> They observed that a dipeptide with the bulkier  $\alpha$ -side chain on the amino ester was obtained in higher yield than a dipeptide where the bulkier  $\alpha$ -side chain is present on the free carboxylic acid amino acid residue. Their results suggested that the first addition to the silyl coupling reagent is that of the free amine residue, and the second, is that of the free carboxylic acid residue. Some monitoring experiments were performed including NMR and MS, which did not show evidence of the tethered intermediate, but control experiments supported their proposed mechanism. Conducting the reaction in the absence of the carboxylic acid coupling partner led to the formation of intermediate **44**, which was confirmed by  $^1\text{H}$  NMR (Figure 45). Subsequent addition of the carboxylic acid formed the amide in 73 % yield after running overnight. These results suggested that the 9-silafluorenyl dichloride-mediated amide bond formation proceeds through the chemical ligation pathway.<sup>60</sup>

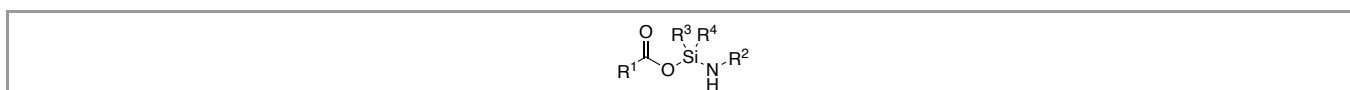


Figure 44 Tethered intermediate proposed by Charette *et al.*

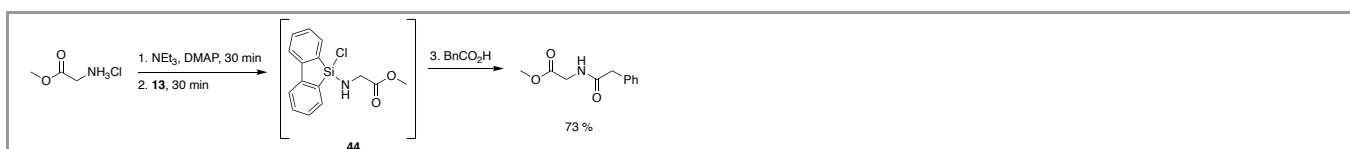


Figure 45 Formation of tethered intermediate **44**.

However, computational data reported by Jiang and Bi *et al.* supports an intermolecular C-N bond formation pathway (Path C) for Charette's method (Figure 46).<sup>79</sup> The calculations for the general reaction were modelled using the coupling of acetic acid with methylamine in the presence of trimethylamine ( $\text{Me}_3\text{N}$ ), DMAP, and **7**. The key silyl amine and silyl ester intermediates **7-C**, **7-N**, **7-CC**, **7-CN**, and **7-NN** (Figure 47) are generated from the coupling of carboxylic acids and amines with **7** through nucleophilic addition of either the carboxylic acid or amine, deprotonation, and dechlorination; nucleophilic addition and deprotonation could also occur via a concerted pathway. It was determined that all the key intermediates are interconvertible because their energy conversions are lower than 20 kcal/mol, which is achievable when heating at 60°C.

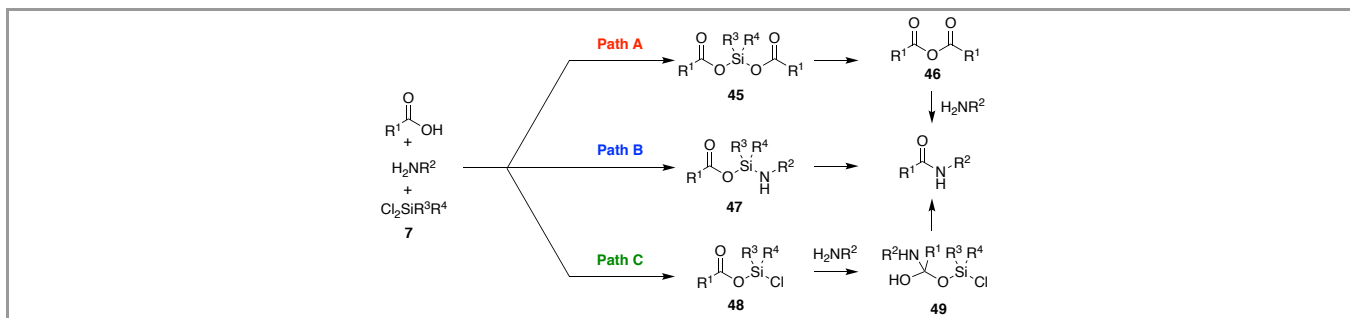


Figure 46 Possible pathways of dichlorosilane-mediated amide bond formation.

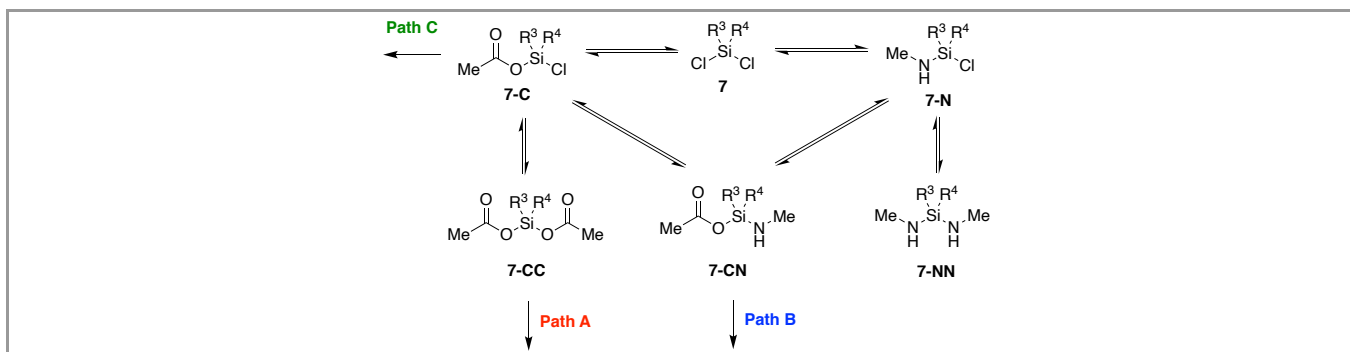


Figure 47 Interconversion between possible silicon tethers.

Jiang and Bi *et al.* then considered the generation of the amide directly from a number of these potential intermediates. Charette and co-workers proposed that an anhydride was a potential intermediate,<sup>60</sup> and this pathway (Path A) was also studied (Figure 48). The direct elimination possessed an inaccessibly high energy barrier; again, however, the unlikely ammonium salt-assisted pathway is possible through **TS-A1**.

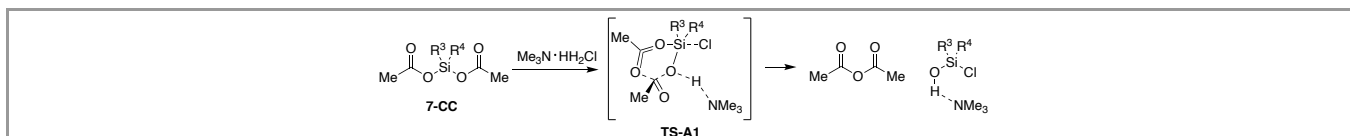


Figure 48 Mechanism for anhydride formation.

From **7-CN**, a direct elimination forming the amide and a silanone (Path B) was considered but was immediately excluded due to a significant free energy barrier and the formation of an unstable silanone. Interestingly, the inclusion of  $\text{Me}_3\text{N}\cdot\text{HCl}$  makes this pathway feasible through **TS-B1** (Figure 49); nevertheless this was concluded to be a less likely pathway.



Figure 49 Mechanism for chemical ligation pathway B.

Finally, the intermolecular nucleophilic addition (Path C) was studied. There were two possible sub-pathways considered for this: 1) carboxylic acid-assisted intermolecular nucleophilic addition (Figure 50) and 2) base-assisted intermolecular nucleophilic addition (Figure 51); the carboxylic acid-assisted intermolecular nucleophilic addition was found to have a lower energy barrier

They concluded that the reaction first generates key intermediates **7-C** and **7-N**, which can lead to **7-CN**, **7-CC**, and **7-NN**, all existing in equilibrium. The direct elimination pathway from **7-CC** (Path A) or **7-CN** (Path B) to generate the anhydride or amide, respectively, are the least likely due the generation of an unstable silanone. Therefore, intermolecular nucleophilic addition on **7-C** catalyzed by the carboxylic acid or base is the most kinetically favourable (Path C). Notably, silanols can be readily polymerized to siloxanes in the presence of a base. This polymerization acts as a thermodynamic driving force for amidation but prevents recycling of the coupling reagent and can consume active Si-X equivalents.

## 4.2 Mechanism of Amidation via Hydrosilanes

The mechanism of diphenylsilane-mediated amide bond formation has also been proposed by both Charette's group and Jiang/Bi *et al.*<sup>26,80</sup> Jiang/Bi propose a mechanism based on computational data,<sup>81</sup> and Charette *et al.* used experimental data to determine the mechanism. It is generally accepted that the reaction proceeds through silyl ester **59** (Figure 52). Three pathways are proposed thereafter: Charette and

co-workers proposed two pathways, Path A and B,<sup>26</sup> and Jiang/Bi *et al.* further propose Path C.<sup>80</sup> Path A travels through **60** and the amide forms through the chemical ligation pathway. Path B gives the amide by nucleophilic substitution of the amine on the carbonyl carbon of **59**. Jiang/Bi *et al.* propose that **63** forms from nucleophilic addition on silyl ester **59**, followed by concerted proton transfer and C-O bond cleavage, leading to a silanol.

First the formation of silyl ester **59** was explored. Silylation of the carboxylic acid could occur through either a stepwise or concerted pathway, however, a stepwise pathway was favoured. The stepwise pathway proceeds through deprotonation of the carboxylic acid, addition of the carboxylate on diphenylsilane, and dihydrogen release.<sup>80</sup> With respect to the amidation process, Path C (Figure 52) was determined to be the most feasible because: 1) it had the lowest overall free energy barrier, 2) does not result in the formation of unstable zwitterion intermediates, such as **64a** (Figure 53), **64b** (Figure 53), and **65** (Figure 54), and 3) a silanol is formed rather than a silanone, providing the thermodynamic driving force.

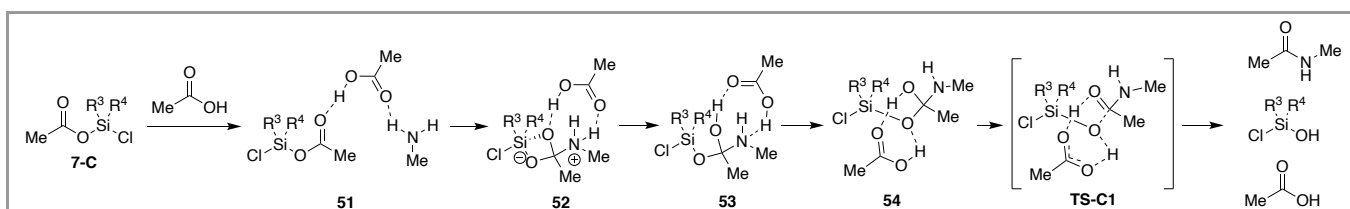


Figure 50 Carboxylic acid promoted path C.

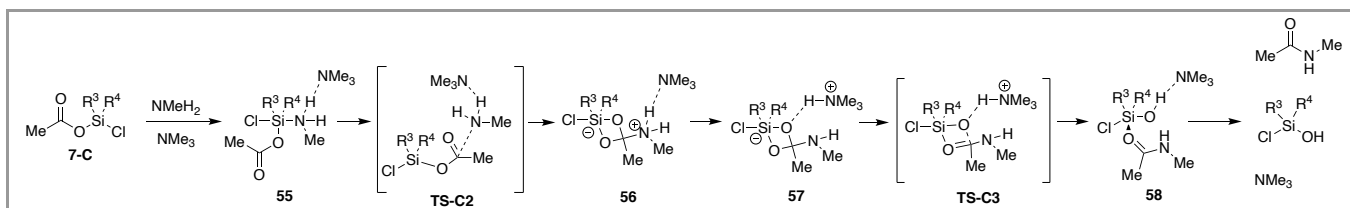


Figure 51 Base promoted path C.

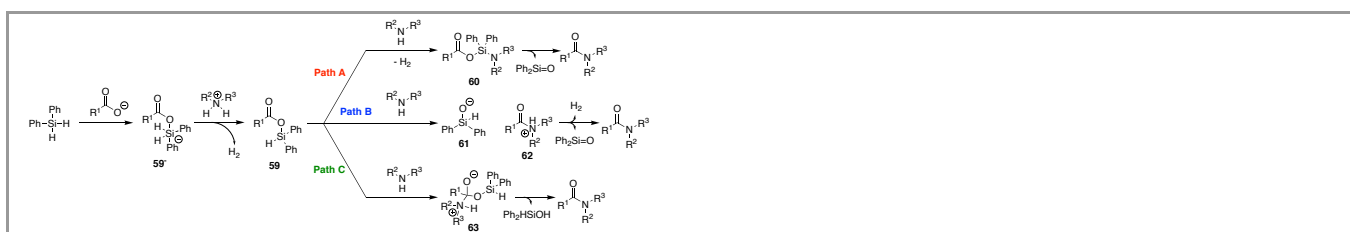


Figure 52 Proposed mechanistic pathways for diphenylsilane-mediated amide synthesis.

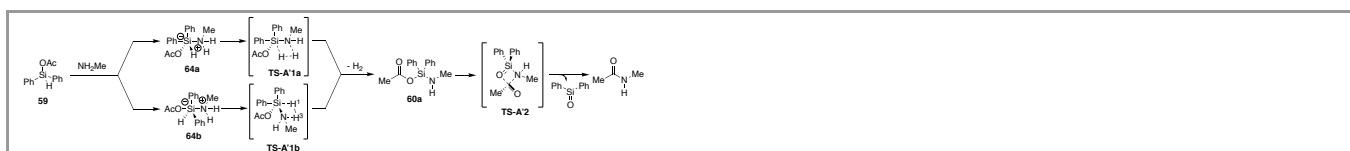


Figure 53 Chemical ligation path A.



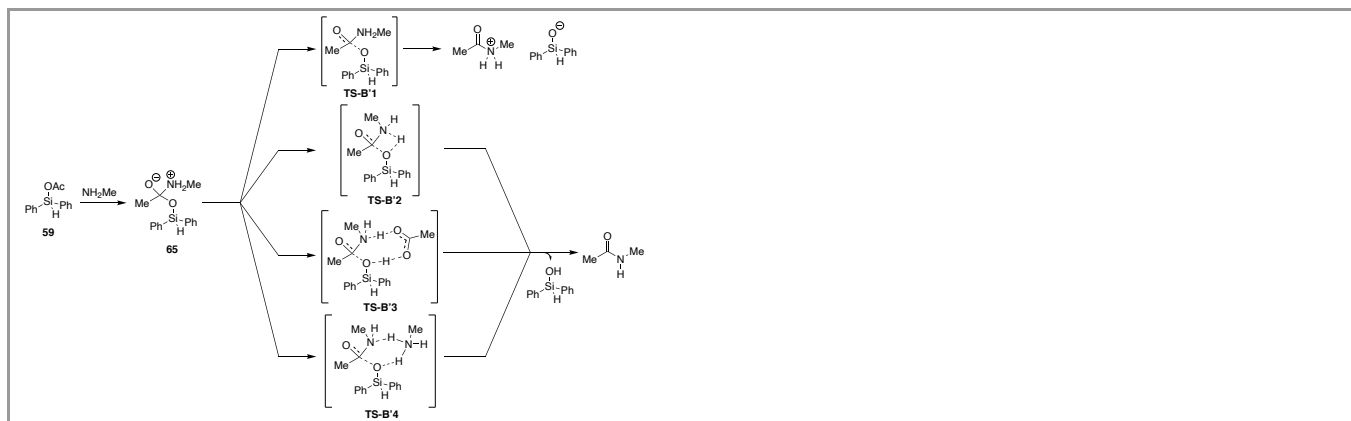


Figure 54 Mechanism of path B.

Path C (Figure 55) begins with a concerted proton transfer and C-N bond formation through **TS-C'1** to generate **66**. In this intermediate, the carboxylic acid can act as a hydrogen bond acceptor and donor to hydrogen bond to the hydroxyl group and amine, respectively. **66** will isomerize to **66'** and the carboxylic acid hydrogen bonds to the silanolate oxygen. From **66'**, a concerted proton transfer and C-O bond cleavage through **TS-C'2** forms the amide and silanol

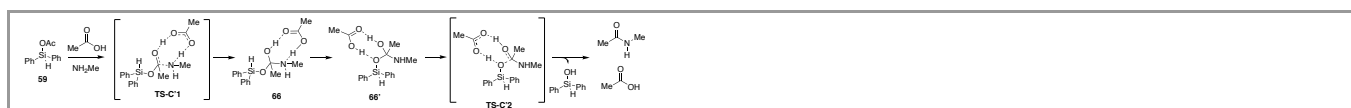


Figure 55 Carboxylic acid assisted nucleophilic addition path C.

The incorporation of an additional acyloxy group on the silane is possible, which forms a bis(acyloxy)silane. Charette and co-workers observed the monoacyloxysilane and amide synthesis worked when using a monohydrosilane,<sup>26</sup> suggesting that the monoacyloxysilane is the reactive silyl ester intermediate. Further, this observation (that amidation can occur from monohydrosilane  $\text{Ph}_3\text{SiH}$ ) seemingly demonstrates that ligation is not required for amidation to occur. Jiang and Bi *et al.* showed that the formation of the bis(acyloxy)silane from the mono(acyloxy)silane is slower than amide formation, so the formation of silyl ester **59** is more kinetically favourable. Although **59** seems to be more likely, the bis(acyloxy)silane is not excluded.

The structure-activity relationships of silanes, carboxylic acids, and amines were studied, and overall energy barriers and energy costs were calculated to investigate their activity in the rate-determining dihydrogen and amide formation (Figure 56).<sup>80</sup> The reaction of acetic acid and  $\text{Me}_3\text{N}$  with different silanes and then the reaction of different carboxylic acids and amines using diphenylsilane were explored.

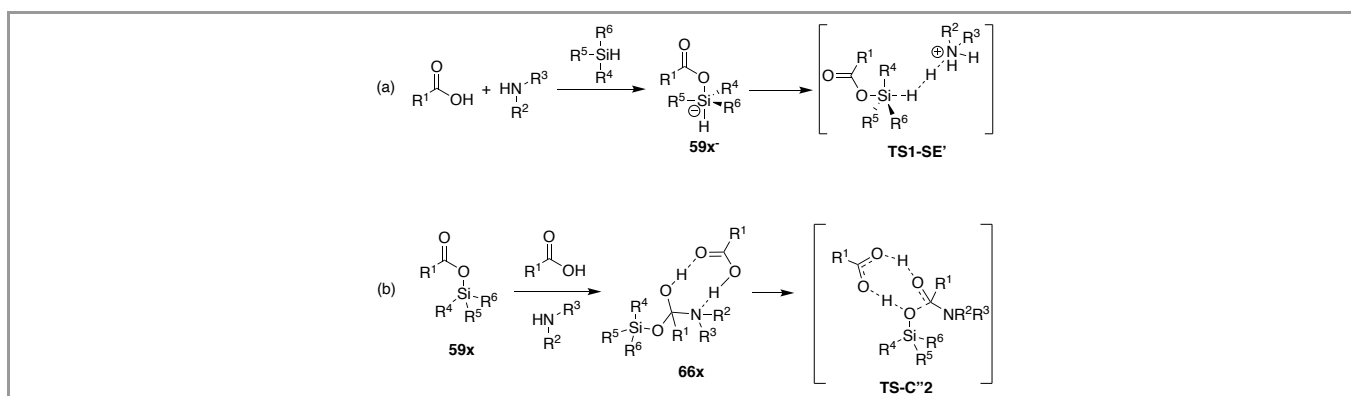


Figure 56 (a) Rate-determining step of dihydrogen formation. (b) Rate-determining step of amide formation.

In general, trisubstituted silanes led to higher overall energy barriers of dihydrogen formation compared to disubstituted silanes, while phenylsilane resulted in the lowest energy barrier, suggesting that this step is mainly controlled by sterics. The amide bond forming step (Figure 56b) is not as influenced by the electronic properties of Si because no bonds attached to the silicon are broken or formed in this step. Overall, less bulky silanes are more reactive. For dihydrogen formation (Figure 56a), more acidic carboxylic acids, such as acetic acid and trifluoroacetic acid, and less bulky acids such as phenylpropionic acid, showed higher reactivity. For the amide forming step, less acidic alkyl carboxylic acids and trifluoroacetic acid have higher reactivity in amide formation. Charette and co-workers' experimental results support this data, but for phenylethynyl acid a low yield was obtained, suggesting possible side reactions. Generally, less bulky, medium basic amines (primary alkyl amines) had the highest reactivity and secondary amines and aniline had slightly lower reactivity.

Blanchet and co-workers concluded that the phenylsilane-mediated reaction does not proceed through the chemical ligation amide synthesis (i.e. intermediate **43**),<sup>79,80</sup> but rather through a diester (**67**) or triester (**68**) formed by dehydrogenative addition of phenylsilane to the carboxylic acids (Figure 57).

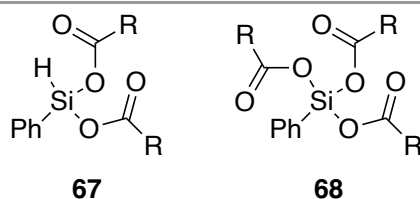


Figure 57 Possible silyl ester intermediates proposed by Blanchet *et al.*

They were unable to isolate any reactive intermediates, and so to test this mechanistic hypothesis they explored the acetylation of morpholine with various silyl acetates (Figure 58). Addition of one equivalent of silicon tetraacetate **34** gave the acetylated morpholine in 99% conversion. They proposed that more acetate groups on the silicon increased the electrophilicity of the carbon of the carbonyl, and amide formation most likely proceeds through silyl ester intermediate **68** when using phenylsilane. (This concept was subsequently applied by using silicon tetraacetate (**34**) as a general acetylating agent of amines (Figure 32c).)

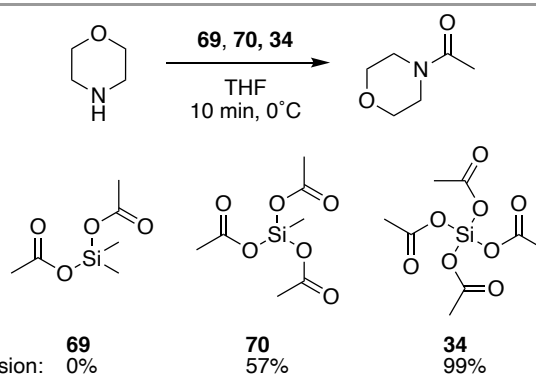


Figure 58 Acetylation of morpholine with different silyl acetates.

### 4.3 Mechanism of Amidation using Oxy-/Azasilanes

In the peptide coupling reaction using Ta(OMe)<sub>5</sub> and 1-(trimethylsilyl)imidazole (**19**), Muramatsu and Yamamoto also describe the formation of a reactive silyl ester intermediate. First, they were able to confirm the presence of silyl ester **69** by <sup>1</sup>H and <sup>29</sup>Si NMR, and subsequently react it with an amino ester to give the corresponding peptide in high yield (Figure 59).

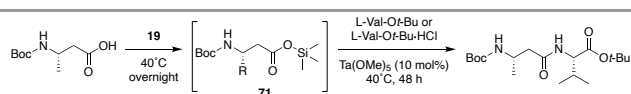


Figure 59 Synthesis of silyl ester **71**.

A proposed reaction mechanism (Figure 60) showed that the protected amino acid (**AA**) first reacts with **19** to produce silyl ester **72**. The carbonyl oxygen of the protecting groups can coordinate to Ta followed by coordination of the carbonyl oxygen of the silyl ester forming **TS-I**. This eight-membered transition state is not very stable, but the activated silyl ester can react with amines to form the amide bond. A tantalum migration is possible to form **TS-II**. Nucleophilic attack by the unprotected amine of the amino ester (**AE**) at the carbonyl carbon of the activated silyl ester in **TS-I** or **TS-II** yields the peptide, and the catalyst is regenerated.

To gain insight into the mechanism of **30**-mediated peptide coupling reported by Muramatsu, Yamamoto, and co-workers, control experiments were completed to investigate a possible silylated amine and silyl ester as reactive intermediates (Figure 61). An *N*-silylated amino ester **73-I** and an *N,N*-disilylated amino ester **73-II** were observed (Figure 61a). **30** also reacted with benzylamine (**74**) to give aminosilane **74-I** (Figure 61a). Silyl esters **75-I** and **76-I** were also obtained (Figure 61b). With the reaction of the carboxylic acids and **30**, different silyl ester coordination structures were observable, including **77**. The mix of silyl esters derived from **75**, reacted with **73** to give the corresponding peptide in 89% yield. If one of the silyl esters is **77**, then it explains the excellent stereochemical integrity because racemization through an oxazolone can be blocked by the formation of a seven-membered ring intermediate.

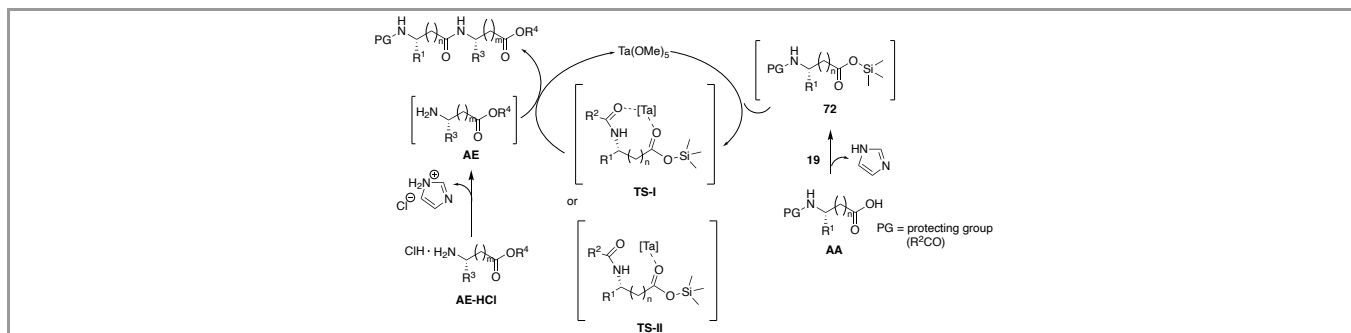


Figure 60 Proposed reaction mechanism using **19** and Ta(OMe)<sub>5</sub>.

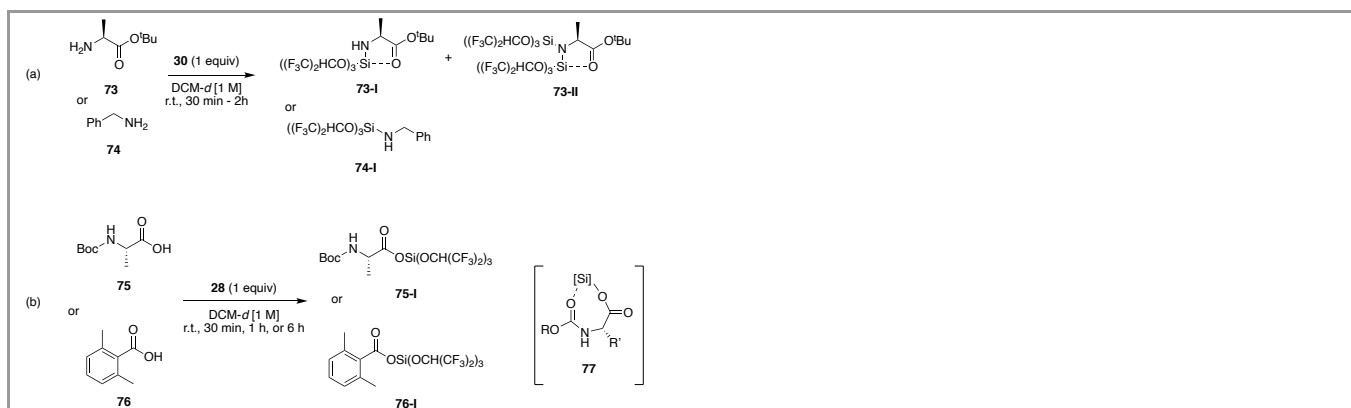


Figure 61 (a) Formation of silylated amino ester and aminosilane. (b) Formation of silyl esters.

The reaction of silylated amine **73-I** with amino acid **75** was shown to be forming the hexacoordinate silicon species **78** (Figure 62). They observed that the hexacoordinate silicon species (e.g. **78**) were consumed slowly over time to form the peptide bond. The *N*-silylated amino ester **73-I** reacted with silyl ester **75-I** to form the dipeptide in good yield.

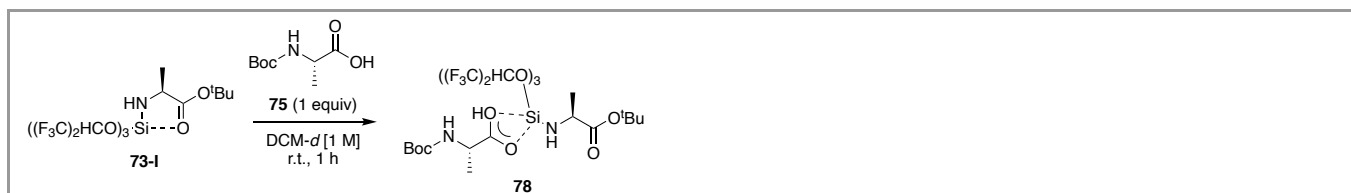


Figure 62 Formation of hexacoordinate silicon species **78**.

The authors propose two plausible mechanistic pathways for their reaction: a minor (blue arrows) and major (red arrows) route (Figure 63). In the minor route, the amino ester (**AE**) initially reacts with **30** to generate **73x-I**. The silicon atom in **73x-I** interacts with the oxygen atoms of the *N*-protected amino acid **AA** to form the hexacoordinate intermediate **78x**. The authors propose the next step is the migration of the silyl group from NH<sub>2</sub> to the carboxyl group followed by amidation to form the peptide. In the major route (red arrows), **30** reacts with the *N*-protected amino acid **AA** to generate the silyl ester **75x-I**. A catalytic amount of **33** or **78'x** can accelerate this step. **75x-I** then reacts with the amino ester or **73x-I** to give the final peptide product.

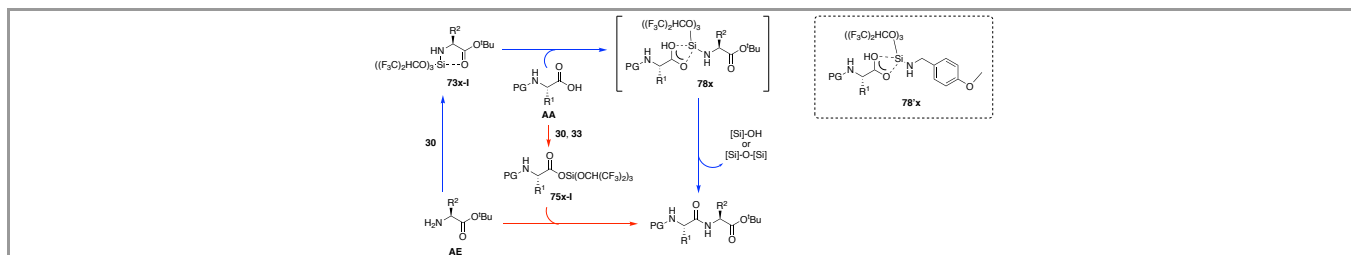


Figure 63 Proposed reaction mechanism – minor (blue) and major (red) route.

A mechanism was proposed for the **30**-catalyzed peptide bond formation using trimethoxysilane **29** (Figure 64).<sup>70</sup> Silyl ester **79** is formed when **30** reacts with a carboxylic acid. This silyl ester reacts with the amine to generate the amide, generating silanol **80**. The

silanol and **31** can react to generate siloxane **81** to form silyl ester **82** that can lead to the amide by reaction with the amine. Mechanistic experiments were performed to gain further insight into the mechanism (Figure 65). NMR experiments showed the presence of trimethoxysilyl ester **83** formed from benzoic acid under optimal reaction conditions. An amino acid was used, and silyl ester **84** formed in a similar manner. This showed that the formation of the trimethoxy silyl ester is part of their pathway.

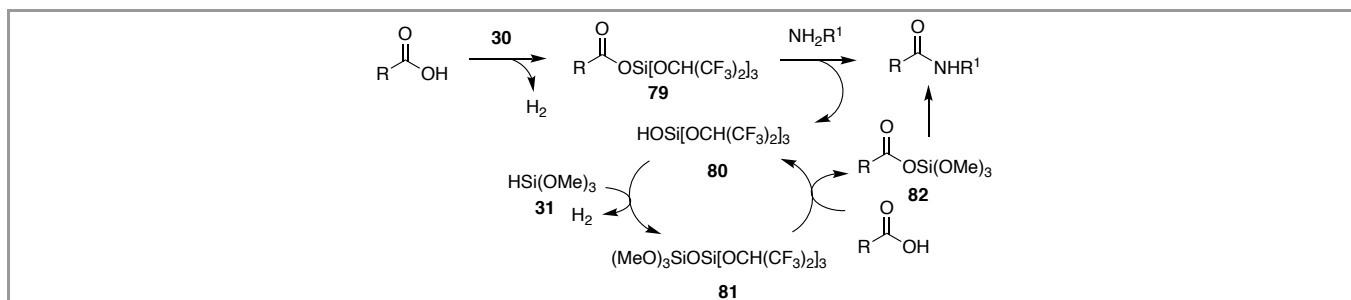


Figure 64 Proposed mechanism of **31**-mediated amide formation.

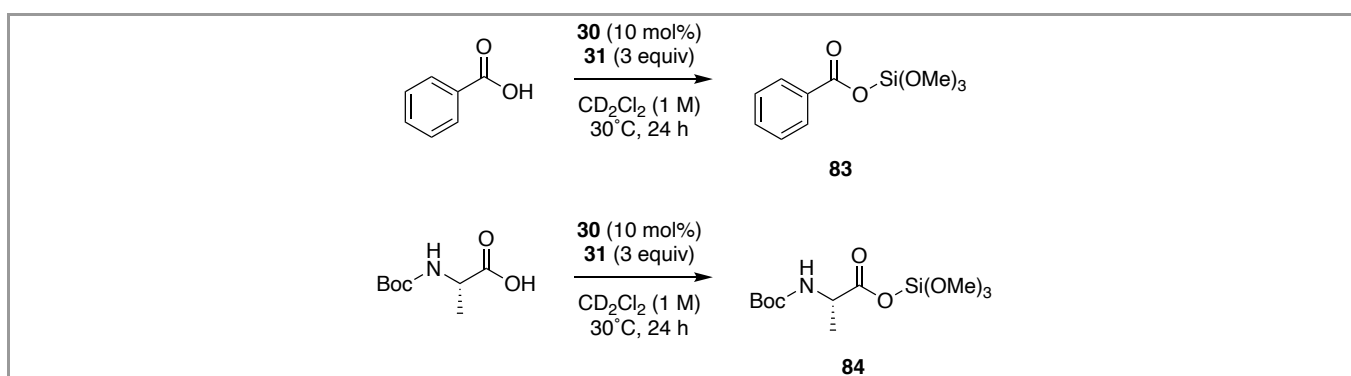


Figure 65 Silyl esters detected by NMR experiments.

Silicon-mediated amide formation undoubtedly proceeds through the formation of silyl ester intermediates as activated carboxylic acids. Following the formation of the silyl ester, two mechanisms are proposed (Figure 42) and have been debated in the literature. Given the current evidence, we conclude that amide formation most likely proceeds through the “carboxylic acid activation” pathway shown in Figure 42. This pathway leads to thermodynamically favourable silanol by-products, in comparison to the chemical ligation pathway, which would directly produce an unstable silanone.

## 5. Making Esters from Silyl Esters

Esters, like amides, are important carboxylic acid derivatives that are present in many drugs, natural products, and polymers. While silyl esters have not been demonstrated as precursors for conventional alkyl or aryl esters, researchers have exploited silyl esters as transient, reactive intermediates in the synthesis of perfluoroalkyl esters<sup>65</sup> and thioesters.<sup>10a,64</sup>

While developing methods for amide synthesis, Mukaiyama and co-workers noted the appearance of a perfluoroester by-product in the reaction using  $\text{Si}[\text{OCH}(\text{CF}_3)_2]_4$  (**22**) as a coupling reagent.<sup>65</sup> When the reaction was run in the absence of a nucleophilic amine, tetrakis(perfluoroalkoxy) silanes directly transformed carboxylic acids into the corresponding perfluoroalkyl esters (Figure 66).  $\text{Si}(\text{OCH}_2\text{CF}_3)_4$  or  $\text{Si}[\text{OCH}(\text{CF}_3)_2]_4$  (**22**) were used in the presence of a base (TEA or DMAP), and the corresponding esters were made in high yield at room temperature.

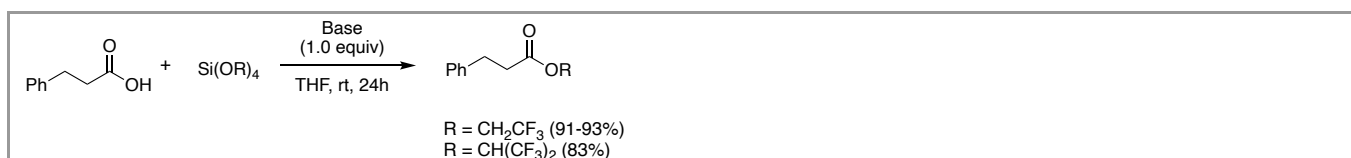


Figure 66 Synthesis of perfluoroalkyl esters.

Mukaiyama and co-workers also investigated the utility of imidazol-1-ylsilane derivatives (**15** or **16**) towards the synthesis of thioesters.<sup>64</sup> They observed that  $\text{Si}(\text{2-Me-Im})_4$  (**16**) could be used to make thioesters from carboxylic acids and thiols (Figure 67a). Thioesterification worked well using **16** at room temperature. The reaction proceeded under mild conditions to afford the corresponding thioesters in good to excellent yields. Muramatsu and Yamamoto also extended their Ta-catalyzed amidation method using **19** for the synthesis of thioesters. With **19** and  $\text{Ta}(\text{OMe})_5$  as a Lewis acid catalyst, they were able to form thioesters from amino acids in good yield (Figure 67b).<sup>10a</sup> These reactions are likely to proceed through the 1-acylimidazole intermediate **18**.

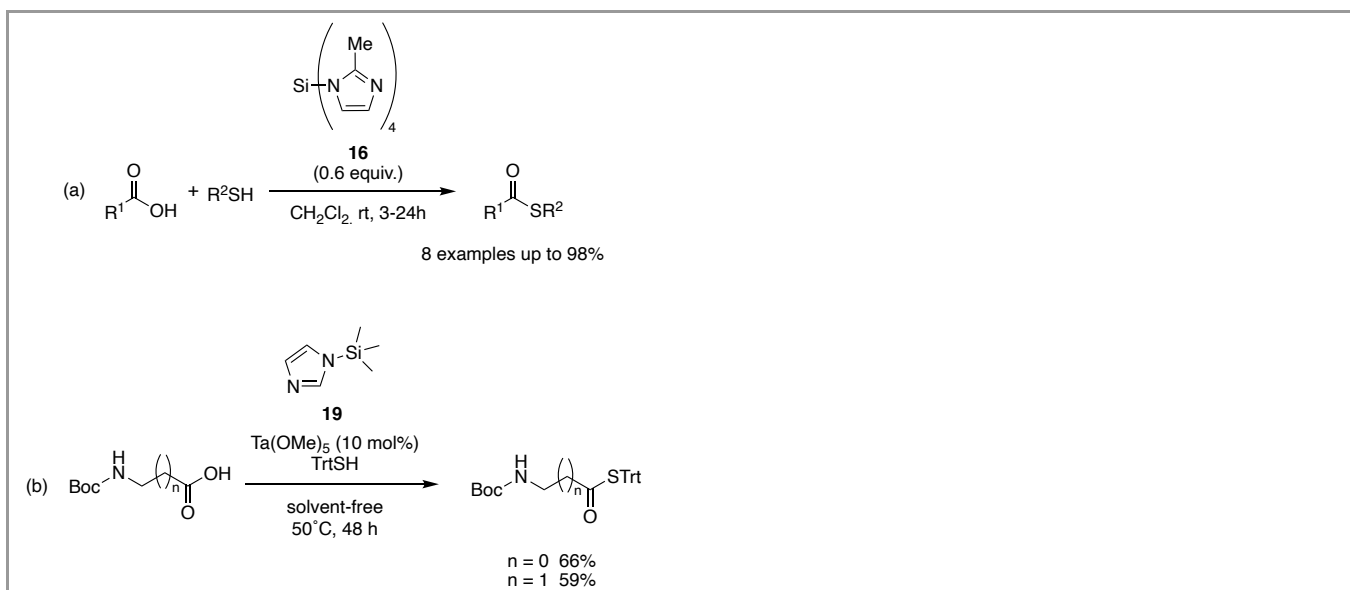


Figure 67 Synthesis of thioesters using: (a) **16** or (b) **19**.

## 6. Making Aldehydes, Alcohols, Amines, and Alkanes *via* Reduction

Carboxylic acids, which are naturally abundant, can be reduced to form many valuable synthetic products and intermediates such as aldehydes, alcohols, or alkanes. Direct reduction of carboxylic acids is challenging and requires strong reducing agents or catalysts to facilitate the reaction. Hydrosilanes, which contain Si-H bonds, are well known hydride sources for the reduction of organic compounds such as carboxylic acids; they are readily available, safer, and a greener alternative to familiar metal hydride sources. Hydrosilanes are particularly useful for the partial reduction of carboxylic acids to aldehydes. In general, the reduction of a carboxylic acid by a hydrosilane proceeds *via in situ* generation of a silyl ester, subsequent reduction of this intermediate to a stable disilyl acetal (**SA**), and then either: 1) formation of the aldehyde (in red), 2) full reduction to the alcohol after hydrolysis of a silyl ether (in blue), or 3) complete deoxygenation (in green) (Figure 68). There are several reports of both metal-free<sup>82-85</sup> and metal-mediated<sup>86-94</sup> hydrosilylation of carboxylic acids, to make a variety of products *via* the reactive silyl ester intermediate.

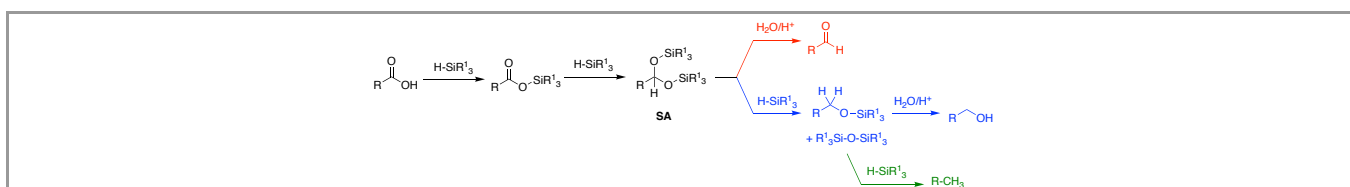


Figure 68 Possible routes of reduction of carboxylic acids by hydrosilanes.

### 6.1 Aldehyde Synthesis by Metal-Free Reduction

In 1984, Corriu, Lanneau, and Perrot reported the uncatalyzed reduction of carboxylic acids to aldehydes through pentacoordinate silyl esters, without any catalysts (Figure 69).<sup>84</sup> Silyl esters **86** are formed upon reaction of a carboxylic acid with pentacoordinate silanes **85a-85c**, and subsequent thermal decomposition of the silyl ester forms the aldehyde, with a cyclic siloxane **87** as the by-product. Silane **85b**, which is coordinated in a six-membered ring, was more reactive compared to **85a** or **85c**; however, in all cases, intramolecular coordination gave enhanced reactivity of the Si-H bond, which was necessary for the reaction to occur. It was proposed that thermal decomposition happens through the elimination of the aldehyde, followed by formation of an unstable silanone (**88**) to give the cyclic siloxane **87**. Many aldehydes were synthesized in good yield, however, harsh and forcing conditions were required.

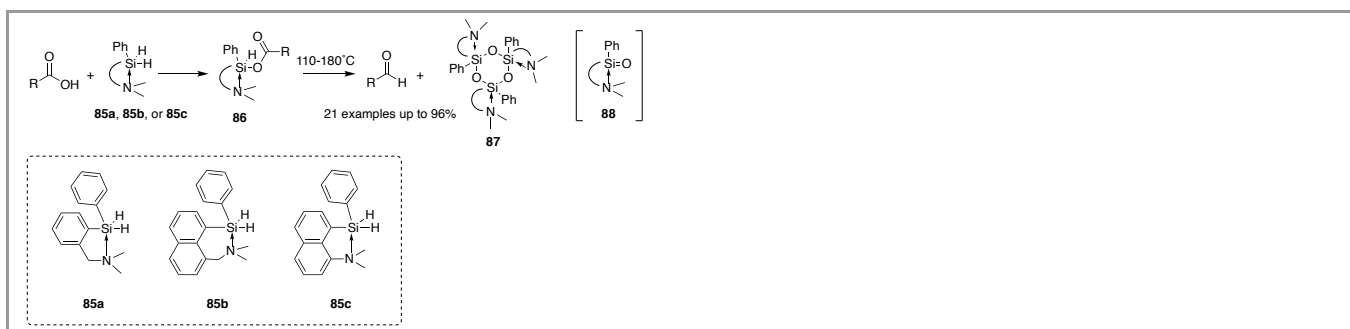


Figure 69 Reduction of carboxylic acids with pentacoordinate silanes.

Brookhart and co-workers were interested in selectively reducing carboxylic acids to aldehydes and report a  $B(C_6F_5)_3$ -catalyzed hydrosilylation of carboxylic acids with silanes under mild conditions.<sup>83</sup> A loading of 0.05 – 2.0 mol % of the borane and tertiary silanes were optimal for reduction (Figure 70). In the reduction of hydrocinnamic acid, a lower catalyst loading decreased the amount of over-reduction (i.e. silyl ethers or deoxygenated products) and full conversion to **89** was obtained. Several aliphatic carboxylic acids were reduced in good to excellent yields to the corresponding disilyl acetal using triethylsilane, however, bulkier aliphatic substrates required phenyldimethylsilane. Aromatic carboxylic acids were reduced using triphenylsilane and 2 mol % of  $B(C_6F_5)_3$ , however, bulkier substrates required the use of triethylsilane. Acidic work-up gave the corresponding aldehydes. The authors then proposed a reaction mechanism for their method (Figure 71). They speculated that first the silyl ester (**90**) forms from the carboxylic acid. They propose that the electrophilicity of the silyl ester is enhanced by coordination to a putative silylium formed by extraction of the hydride from the silane by  $B(C_6F_5)_3$ . Other methods exist for the  $B(C_6F_5)_3$ -catalyzed reduction of carboxylic acids with alkylsilanes, however, no silyl ester intermediate is reported.<sup>95,96</sup>

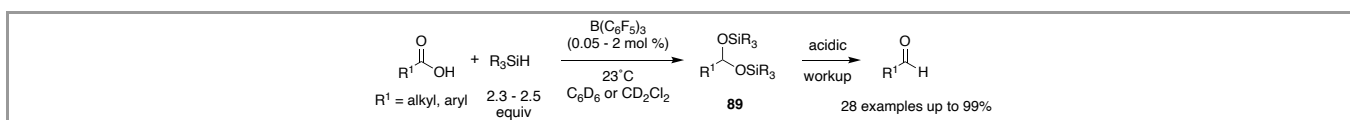


Figure 70 Reduction of carboxylic acids proposed by Brookhart and co-workers.

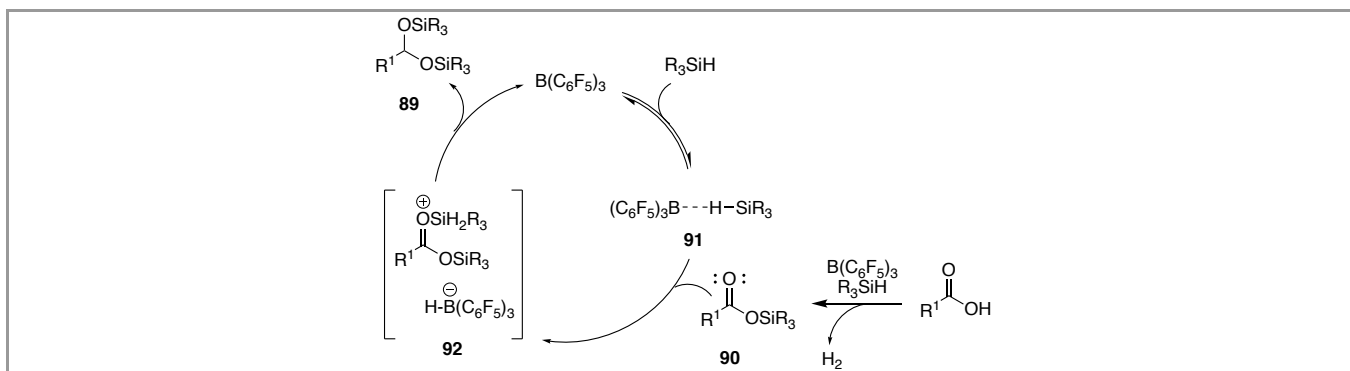


Figure 71 Mechanism of  $B(C_6F_5)_3$  catalyzed reduction of carboxylic acids.

## 6.2 Aldehyde Synthesis by Metal-Mediated Reduction

Diisobutylaluminum hydride (DIBAL-H) was used by Chandrasekhar and co-workers for the direct conversion of carboxylic acids to aldehydes by chemoselective reduction of their corresponding *in situ* generated trimethylsilyl esters **93** (Figure 72).<sup>87</sup> The carboxylic acids were treated with  $Et_3N$  and trimethylchlorosilane to form the silyl ester intermediate **93**; subsequent addition of DIBAL-H provided aldehydes in excellent yields. In addition to the use of a hazardous aluminum hydride reagent, the reduction step needed to be conducted at low temperatures.

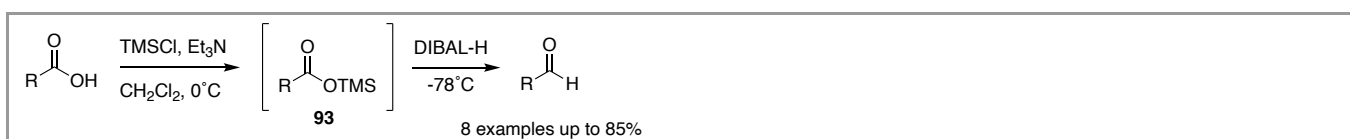


Figure 72 Reduction of trimethylsilyl esters **93** using DIBAL-H.

Nagashima and co-workers report the selective reduction of carboxylic acids to aldehydes (Figure 73).<sup>89</sup> In this work, they used 1,2-bis(dimethylsilyl)benzene (**95**) with a catalytic amount of **94** to produce the cyclic disilyl acetal (**96**). The reactions were carried out by adding the carboxylic acid to a mixture of **94** and **95** to form the disilyl acetal, which was hydrolyzed to yield the aldehyde. The disilyl acetals **96a** and **96b** (Figure 74) were isolated and provided evidence for the formation of the cyclic intermediates (**96**). NMR experiments and mass spectrometry confirmed the structure of **96a** and an X-ray structure confirmed the formation of **96b**. The cyclic disilyl acetal **96** is rigid and the steric hindrance added from the methyl groups on the silicon protects the acetal from further attack, which inhibits further reduction.

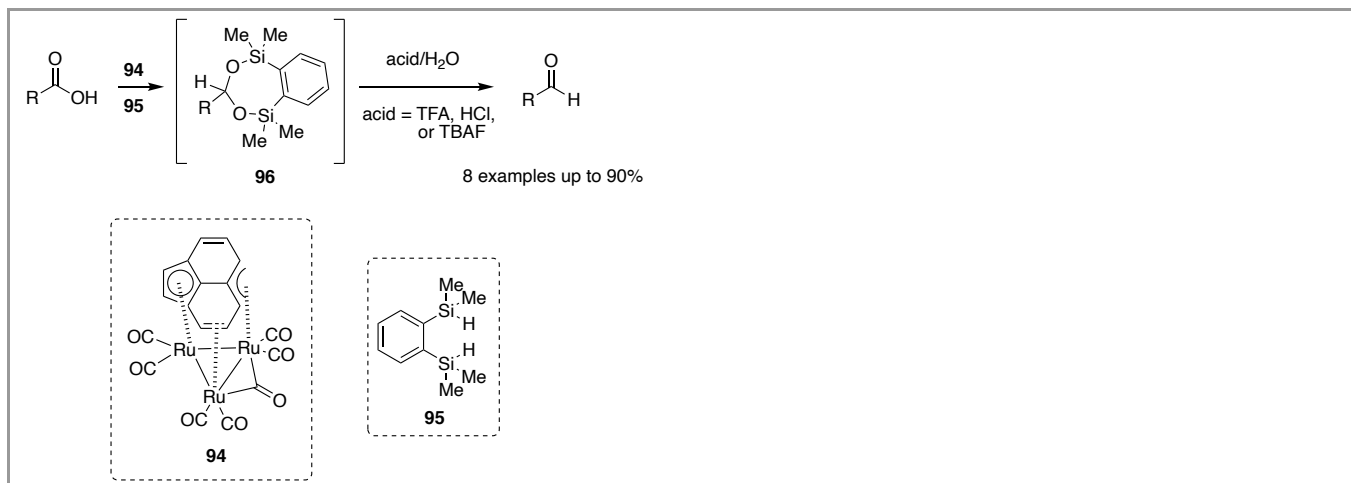


Figure 73 **94**-catalyzed selective reduction of carboxylic acids using **95**.

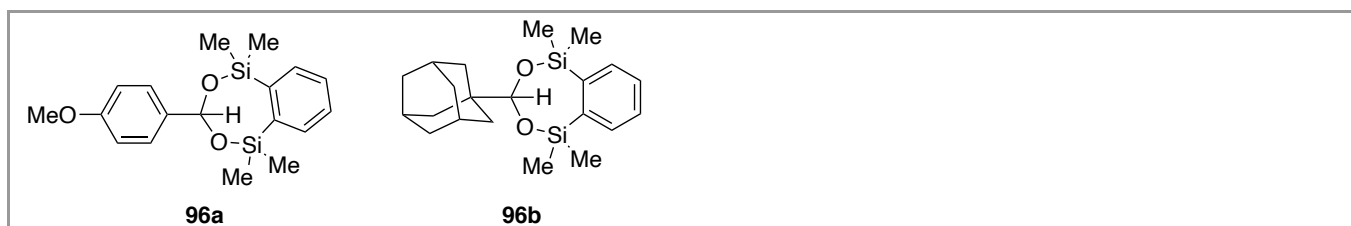


Figure 74 Disilyl acetals used to confirm structures.

In 2019, Sortais and co-workers developed a Re(I)-catalyzed reduction under irradiation at either 350 nm or 395 nm.<sup>94</sup> The authors found high selectivity and yield when using  $\text{Re}_2(\text{CO})_{10}$  with triethylsilane. The observed product was the disilyl acetal (Figure 75), which could then be treated with acid to give the aldehyde. Kinetic studies showed that prior to acetal formation, a silyl ester intermediate **97-I** is observed. Good yields were observed for various carboxylic acids, and more challenging aromatic substrates could be reduced with diphenylmethylsilane in place of triethylsilane (Figure 76).

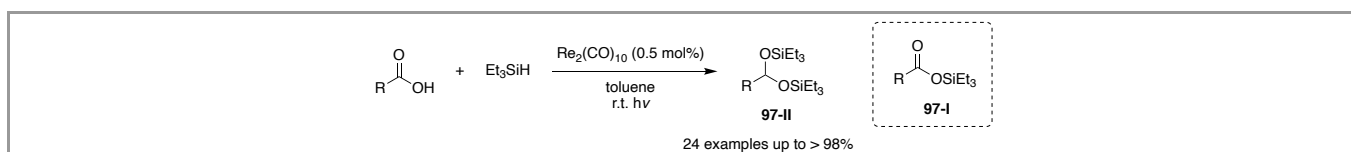


Figure 75 Reduction of carboxylic acids catalyzed by  $\text{Re}_2(\text{CO})_{10}$ .

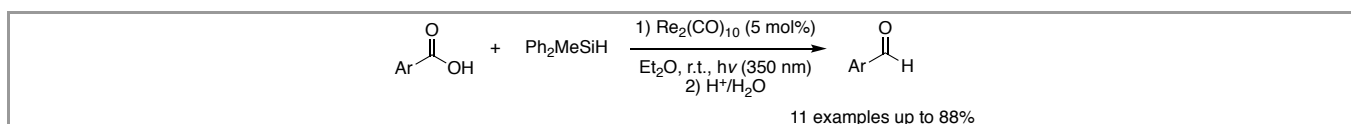


Figure 76 Reduction of aromatic carboxylic acids catalyzed by  $\text{Re}_2(\text{CO})_{10}$ .

Darcel, Sortais, and co-workers investigated the reduction of carboxylic acids to aldehydes utilizing a manganese complex ( $\text{Mn}_2(\text{CO})_{10}$ ) (Figure 77).<sup>92</sup> After optimization studies, high yielding conversion to the disilyl acetal **97-II** was achieved with 5 mol% catalyst,  $\text{Et}_3\text{SiH}$ , and UV irradiation. No over reduction to the silyl ether or fully reduced alkyl product was observed. Various carboxylic acids were reduced in moderate to excellent yields.

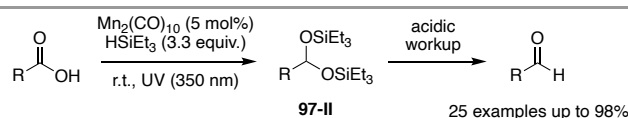


Figure 77  $\text{Mn}_2(\text{CO})_{10}$ -catalyzed selective reduction of carboxylic acids.

Parcel, Sortais, and co-workers also developed methods using iron for the catalytic hydrosilylation of carboxylic acids.<sup>91</sup> They were able to obtain the alcohol, but they noticed that the amount of aldehyde produced increased when using TMDS (1,1,3,3-tetra-methyl-disiloxane), and subsequently found that performing the reaction with (*t*-PBO)Fe(CO)<sub>3</sub> **98** and TMDS gave selective conversion to the aldehyde (Figure 78). Mechanistic investigations with TMDS showed the formation of an open disilyl acetal (**99-O**) intermediate rather than a cyclic disilyl acetal **99-C** (Figure 79). The open disilyl acetal intermediate **99-O** was observable by MS and NMR. This observation is consistent with the requirement of 2 equivalents of TMDS for full conversion and the stability of the disilyl acetal is important to allow for aldehyde formation upon acidic workup. This 6-membered ring closed intermediate **99-C** contrasts with the cyclic intermediate **96** reported by Nagashima and co-workers, which favoured a rigid 7-membered ring intermediate.<sup>89</sup>

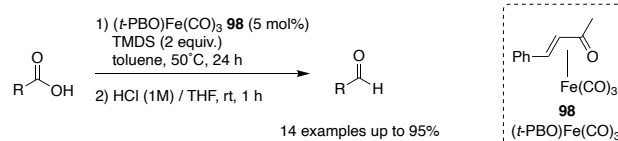


Figure 78 **108**-catalyzed hydrosilylation.

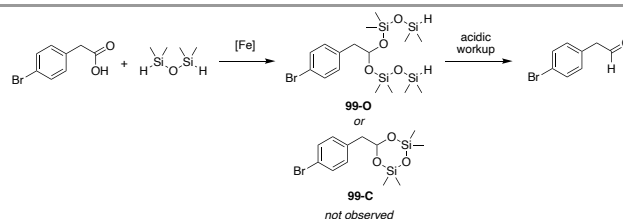


Figure 79 Open and closed disilyl acetal intermediates.

### 6.3 Alcohol Synthesis by Metal-Mediated Reduction

As early as 1967, Venkateswaran and Bardos reported the reduction of silyl esters of amino acids using lithium aluminum hydride ( $\text{LiAlH}_4$ ) to synthesize amino alcohols (Figure 80).<sup>86</sup> The amino acid (**100**) reacts with trimethylchlorosilane in the presence of triethylamine to form the trimethylsilyl ester **101**. Reduction of **101** with  $\text{LiAlH}_4$  formed an *N*-trimethylsilylamino alcohol intermediate **102**, which can be heated with excess water to give the unprotected amino alcohol **103**. In addition, no racemization was observed, but a hazardous and strong aluminum hydride reagent was required.

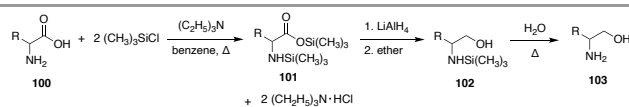


Figure 80 Reduction of silyl esters of amino acids.

In 2002, Nagashima and co-workers used a Ru catalyst for the reduction of carboxylic acids and derivatives using a trialkylsilane.<sup>88</sup> A triruthenium carbonyl cluster (**104**) was found to be an effective catalyst for these transformations (Figure 81). Carboxylic acids were reduced to their corresponding silyl ethers and hydrolyzed to an alcohol, amides were reduced to amines, and esters were reduced to either the silyl ether or alkyl ether (Figure 81).

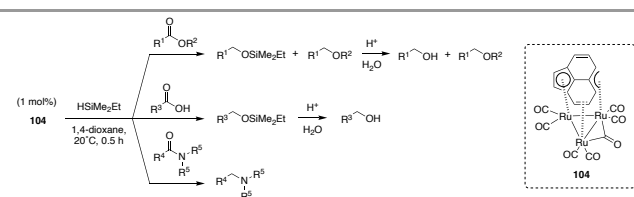


Figure 81 Reduction of esters, carboxylic acids, and amides using  $\text{HSiMe}_2\text{Et}$  and **104**.

In 2014, Fernández-Salas, Manzini, and Nolan synthesized a ruthenium catalyst **105** and developed a method for hydrosilylation



of carboxylic acids to alcohols (Figure 82).<sup>90</sup> The method was chemoselective and potentially reducible functional groups were not reactive under these conditions. The proposed mechanism for this reaction involved a silyl ester intermediate (**106-I**) that is reduced to the disilyl acetal **106-II** and further transformed to either aldehyde or alcohol (Figure 83a). The authors demonstrated that **105** can be used to make a silyl ester using phenyldimethylsilane through dehydrogenative coupling (Figure 83b). It is assumed that the silane is activated by the metal complex through oxidative addition.

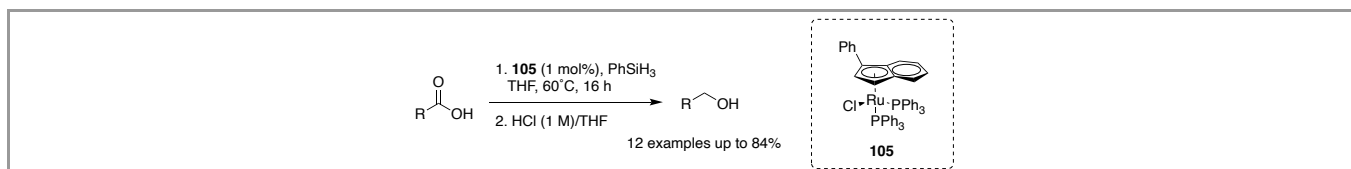


Figure 82 Phenylsilane-mediated reduction of carboxylic acids catalyzed by **105**.

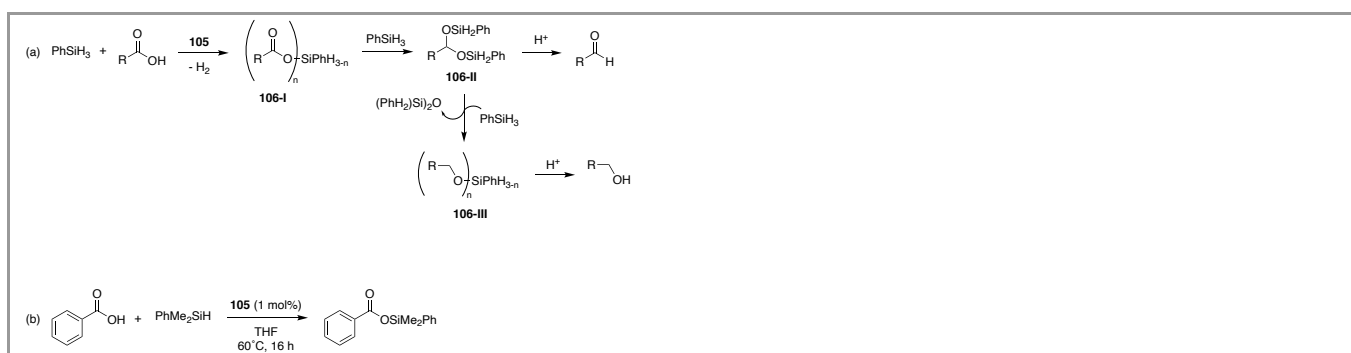


Figure 83 (a) Proposed pathway. (b) Formation of silyl ester using phenyldimethylsilane and **105**.

Darcel, Sortais, and co-workers also developed their method using iron for the catalytic hydrosilylation of carboxylic acids to alcohols.<sup>91</sup> Optimal conversion to the alcohol was observed using  $\text{PhSiH}_3$  in the presence of 5 mol% of  $(\text{CO})_3\text{Fe}(\text{COD})$  **107** under UV-irradiation (350 nm) (Figure 84).

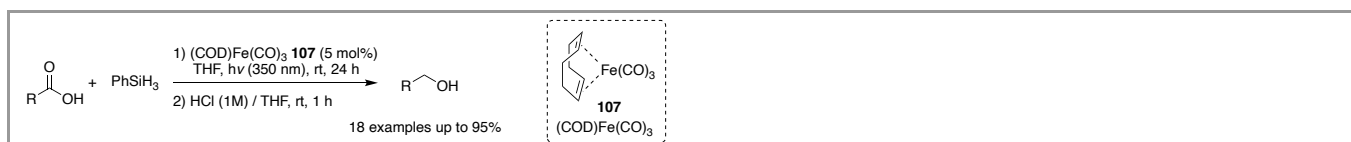


Figure 84 **107**-catalyzed hydrosilylation.

Recently, Werlé and co-workers used a  $\text{Mn}(\text{Br})(\text{CO})_5$  complex for the reduction of carboxylic acids to alcohols.<sup>93</sup> The authors reported optimal reaction conditions using commercially available  $\text{MnBr}(\text{CO})_5$  in 2-methyltetrahydrofuran (2-MTHF) at 80°C using  $\text{PhSiH}_3$ . Various carboxylic acids, including aliphatic and aromatic acids, were reduced and yielded the corresponding alcohol after hydrolysis (Figure 85). Potential reducible functional groups such as alkenes were tolerated, and some heterocycles were also tolerated. Biologically active aryl propionic acids were reduced without compromising chiral integrity. The reaction was also performed on a larger scale without loss of efficiency.

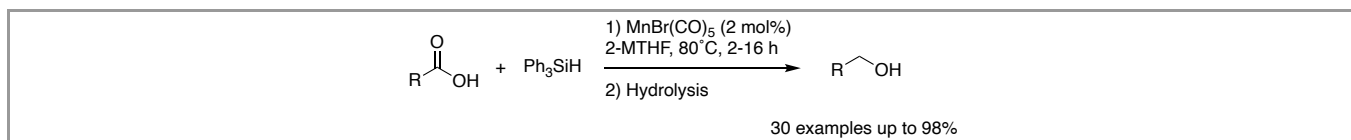
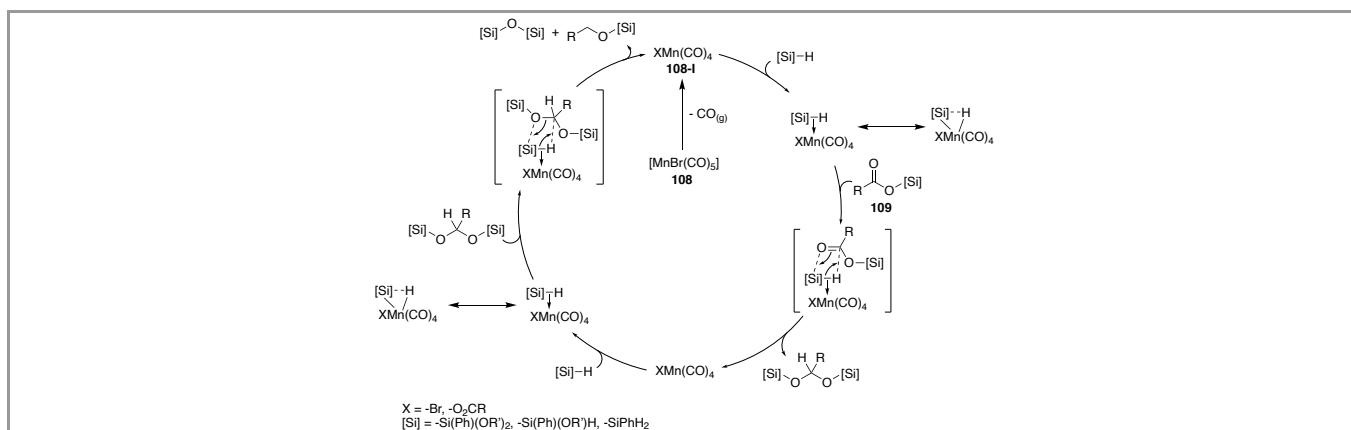
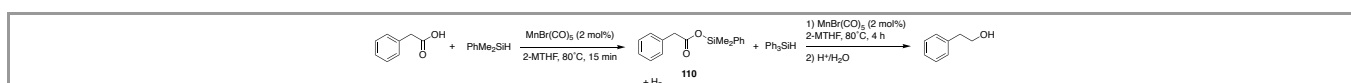


Figure 85  $\text{Mn}(\text{Br})(\text{CO})_5$ -catalyzed reduction of carboxylic acids.

The authors propose that the  $\text{Mn}(\text{I})$  carbonyl complex (**108-I**) as the active species involved in Si-H bond activation through coordination. A proposed catalytic cycle can be seen in Figure 86. Vigorous gas evolution was detected at the beginning of the reaction suggesting dehydrogenative coupling of  $\text{PhSiH}_3$  and the carboxylic acid to form a silyl ester (**109**).  $\text{H}_2$  was identified by GC-TCD and does not participate in reduction as it is released to the atmosphere.  $\text{PhMe}_2\text{SiH}$  reacted with phenylacetic acid to give the corresponding silyl ester (**110**) (Figure 87). It was determined that the Mn complex was necessary to catalyze this step. The silyl ester **110** was reduced by  $\text{PhSiH}_3$  to give the alcohol product in 82% yield. Gas phase composition of the reactions revealed formation of CO, and the authors suggest dissociation of one of the CO ligands upon activation of the catalyst to generate a  $\text{MnX}(\text{CO})_4$  complex (**108-I**).



**Figure 86** Proposed catalytic cycle of Mn-catalyzed hydrosilylation by Werlé *et al.*



**Figure 87** Formation of silyl ester **110**.

In 2021, Denton and co-workers reported a carboxylic acid reduction that was predicated on the deliberate generation of silyl esters, which are believed to function as activated carboxylic acids and enhanced reductants that potentially generate zinc-hydride species upon exposure to zinc acetate (Figure 88). It was demonstrated that, in the presence of zinc acetate and *N*-methylmorpholine, a wide range of carboxylic acids were reduced to the corresponding alcohols. The reduction can be carried out in conventional laboratory glassware and does not require strict exclusion of air or moisture.<sup>97</sup> Reaction monitoring by <sup>19</sup>F NMR spectroscopy demonstrated that, as expected, a complex mixture of silyl esters is generated in the reaction which are reduced to silyl ethers and, upon workup, give the alcohol products (Figure 89). In the presence of *N*-methylmorpholine the silyl esters were observed to form very rapidly (complete within an hour) from the acid and converted into silyl ethers under the reaction conditions after ten hours. In the absence of *N*-methylmorpholine, some silyl ester formation takes place but after ten hours the acid starting material is still visible and no silyl ethers were present. This reduction process highlights how knowledge of silyl ester generation and reactivity can be harnessed to develop new practical synthesis methods.<sup>97</sup>

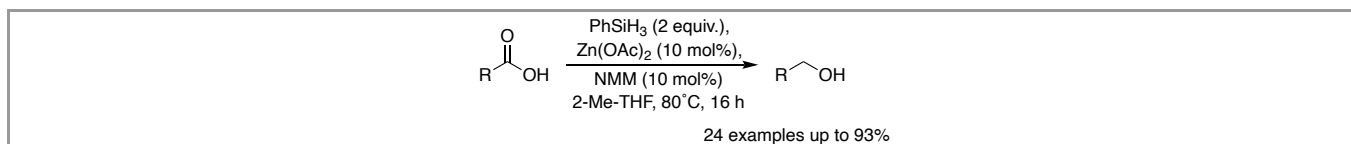


**Figure 88** Zn-catalyzed reduction of carboxylic acids enabled by silyl ester formation.

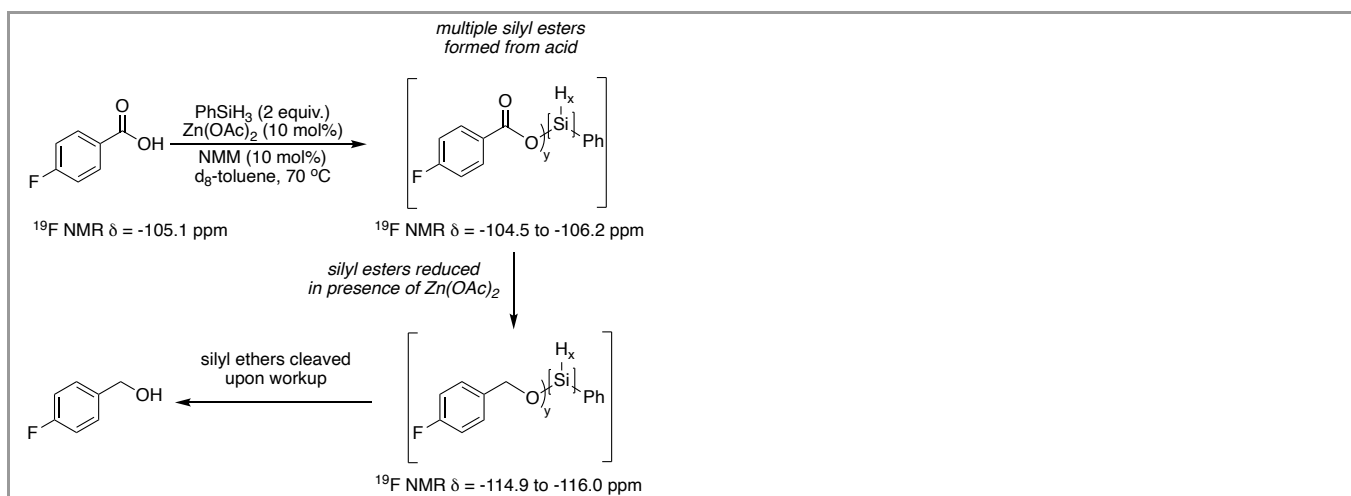


**Figure 89** Zn-catalyzed reduction of carboxylic acids enabled by silyl ester formation.

#### 6.4 Amine Synthesis

In 2017, Denton and co-workers reported a catalyst-free method to access  $\beta$ -fluoroalkylamines using trifluoroacetic acid (TFA).<sup>85</sup> Using this method, secondary amines were trifluoroethylated in good yields (Figure 90). They also performed a three-component reaction

with a primary amine, aldehyde, and TFA to synthesize tertiary amines (Figure 91). First, reductive amination of an aldehyde and primary amine forms the secondary amine (**111**), and then trifluoroethylation occurs. This method exhibited good functional group tolerance, but in some cases double aldehyde addition to the primary amine caused over-alkylation. They proposed (Figure 92) that this occurs through silane-mediated reduction of *in situ* generated silyl ester intermediates from TFA. Initially, dehydrogenative silyl ester formation occurs to generate a mixture of silyl esters **112**, which they observed after conducting mechanistic experiments in the reaction of Et<sub>3</sub>N, phenylsilane, and TFA (Figure 93). The silyl esters can then generate the amide or amine product. Using excess acid, the amine is protonated, and the silyl esters are reduced to silyl acetals or hemiacetals (**113**). The silyl acetals **113** were observed after 24 h from the silyl esters (Figure 93). An equilibrium with the amine is proposed forming an iminium ion **114**. Reduction of the iminium by the silane gives the final trifluoroethylated product. When only 1.0 equivalent of TFA is used, the free amine forms a trifluoroacetamide from the silyl ester intermediates that act as activated acids before reduction. Amide reduction was ruled out as a plausible mechanism because mechanistic experiments show that in the trifluoroethylation of piperidine in the presence of fluoroacetamide resulted in complete recovery of the added amide (Figure 94). Mechanistically this method contrasts with Denton's previously reported *N*-alkylation methods,<sup>24,76</sup> which proceed through amide reduction.

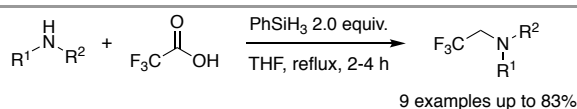


Figure 90 Trifluoroethylation of secondary amines.

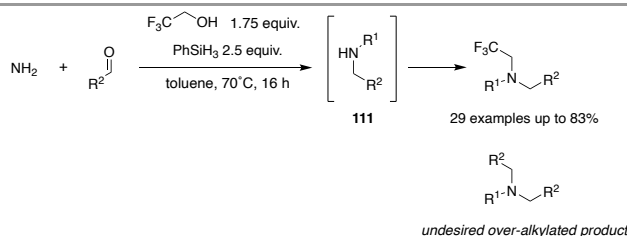


Figure 91 Three-component reaction to make tertiary amines.

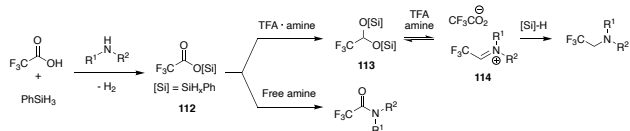


Figure 92 Key intermediates in the trifluoroethylation of amines proposed by Denton and co-workers.

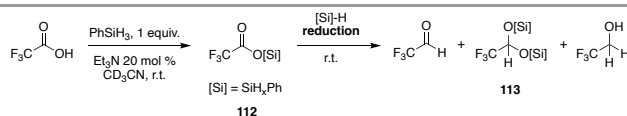


Figure 93 Reduction of TFA-derived silyl ester intermediates.

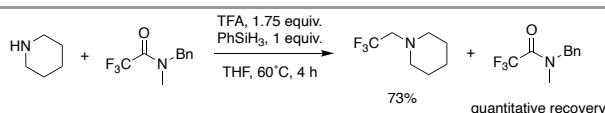


Figure 94 Trifluoroethylation with exogenous amide.

## 6.5 Alkane Synthesis by Metal-Free Reduction

In 2001, Yamamoto and Gevorgyan *et al.* presented a method for the direct conversion of aliphatic carbonyl compounds into alkanes with triethylsilane and B(C<sub>6</sub>F<sub>5</sub>)<sub>3</sub> as a Lewis acid catalyst.<sup>82</sup> Aliphatic aldehydes, acyl chlorides, and esters were reduced efficiently into their corresponding alkane (Figure 95). High yields were obtained in the synthesis of various alkanes from their corresponding aliphatic acids. Deoxygenation of aromatic carboxylic acids was surprisingly challenging and decreasing the equivalents of triethylsilane allowed the partial reduction of such substrates to their triethyl silyl ethers to occur in high yield. The method was not chemoselective as other functional groups present on the substrates such as ketones, acetals, and nitriles were reduced. The authors hypothesized the key intermediates for these transformations (**97-I**, **97-II**, and **97-III**) (Figure 96), which was supported by the detection of several intermediates by GC-MS.

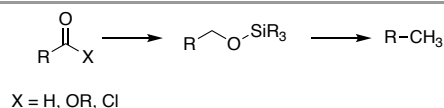


Figure 95 Reduction of aldehydes, esters, and acid chlorides.

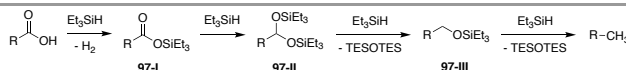


Figure 96 Direct reduction of carboxylic acids to aldehydes.

## 7. Making Acid Chlorides from Silyl Esters

The unique reactivity of silyl esters allows access to a variety of carboxylic acid derivatives and functional groups not yet discussed, including synthesis of acid chlorides.<sup>98</sup> In 1978, Wissner and Grudzinskas investigated the reaction of *tert*-butyldimethylsilyl ester **115**, which is a known protecting group, and oxalyl chloride with substoichiometric amount of DMF to form acid chlorides under neutral conditions with the only by-products being carbon dioxide, carbon monoxide, and *tert*-butyldimethylchlorosilane (Figure 97). The by-products are volatile and easily removed from the reaction.<sup>98</sup> The method was used to synthesize various acid chlorides, which could then be reacted with ethanol and pyridine to form the corresponding ethyl ester. Studying the reaction scope showed that acid-sensitive functional groups were well tolerated. Hydroxy acids can be used in these reaction conditions through simultaneous acid chloride formation and alcohol protection by silylation. The reaction was slow in the absence of DMF, and so the authors propose that the reactive species is the DMF-derived chloromethaniminium **116**, which could add to the carboxyl group of the silyl ester **115** (Figure 98). Intermediate **117** undergoes rearrangement to form the acid chloride.<sup>98</sup>

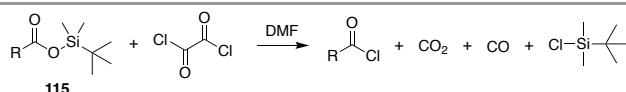


Figure 97 Formation of acids chlorides from **115** and oxalyl chloride.

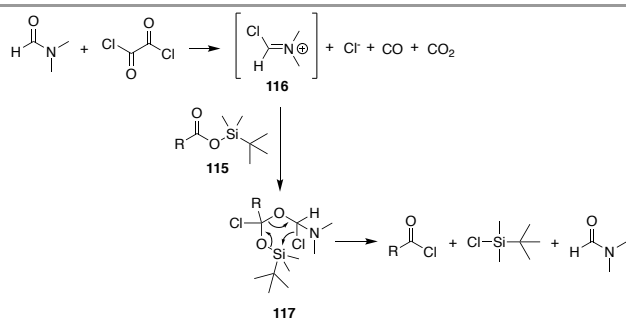


Figure 98 Acid chloride synthesis from **115** and oxalyl chloride in DMF.

## 8. In Situ Generated Silyl Esters and Ramifications for Catalysis

The previous sections of this review have focused upon reactions that are explicitly mediated by silyl ester intermediates and how the diverse reactivity of these species underpin a variety of useful chemical transformations. In this final section we draw attention to reactions in which hydrosilanes and Bronsted acids are present, along with base, where *silyl ester intermediates are not explicitly sought, but are very likely present*. There are an increasing number of reactions in which silyl ester hypotheses are neglected or underappreciated.<sup>99</sup> Most commonly, this occurs when phenylsilane is used as a terminal reductant or dehydrant. In order to present a focused discussion, we examine a subset of catalytic reactions that involve phenylsilane as the terminal reductant and carboxylic acids or carboxamates as the modifiers. It is our hope that an increased understanding of *in situ* silane modification will lead to greater mechanistic understanding and provide a framework for the development of new reactions based upon in situ generated silyl esters.

The catalytic Staudinger ligation is one example of this. The Staudinger amidation reaction is the phosphine-mediated amidation between free acids and azides, reported by Garcia and co-workers in 1984.<sup>100</sup> Triphenylphosphine oxide is an unwanted by-product of this reaction, and in 2012 Ashfeld and co-workers reported a catalytic, traceless Staudinger ligation reaction using a free carboxylic acid, azide, phenylsilane, and catalytic triphenylphosphine.<sup>72</sup> Ashfeld proposed a reaction mechanism (Figure 99) involving the reactive intermediates, aminophosphonium carboxylate (**118**) and *N,O*-phosphorane (**120**). This was followed by chemoselective silane-mediated phosphine reduction to regenerate the phosphine catalyst. In 2017, mechanistic insights into the catalytic Staudinger amidation were reported by Andrews and Denton,<sup>73</sup> and later in 2019 White and Mecinović *et al.* investigated the reaction through NMR experiments to elucidate another plausible mechanism.<sup>74</sup>

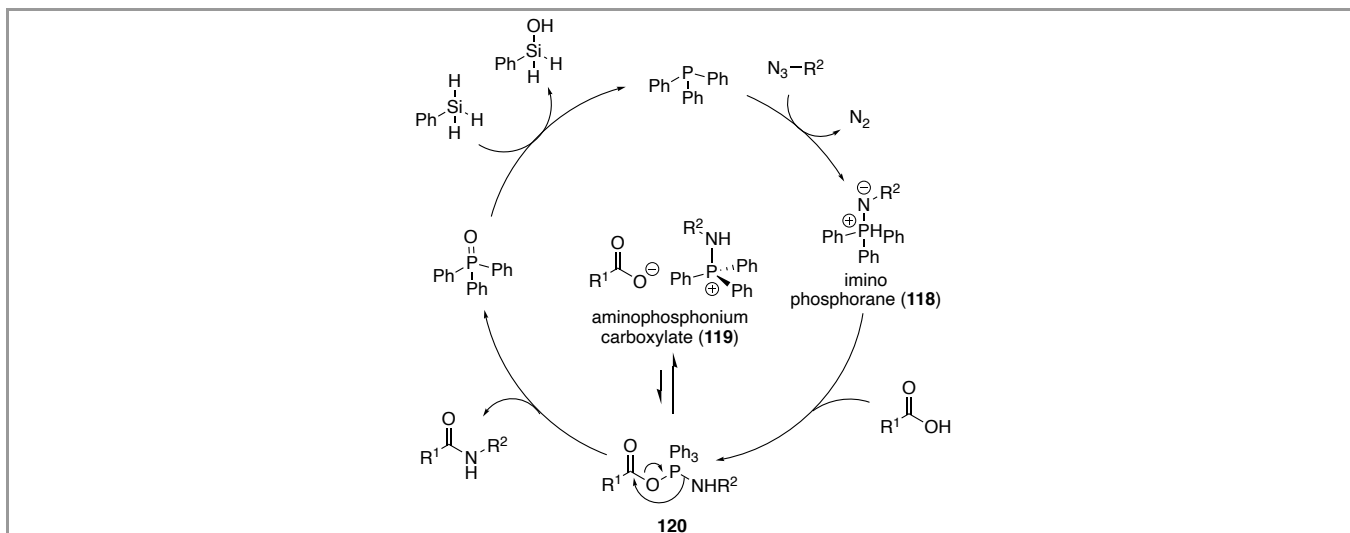


Figure 99 Ashfeld and co-workers proposed mechanism.

Andrews and Denton proposed that this reaction proceeds through reactive silyl ester intermediates. Monitoring the reaction of benzyl azide and triphenylphosphine by  $^{31}\text{P}$  NMR showed the expected iminophosphorane **118** and triphenylphosphine oxide. After benzoic acid was added to the reaction, the aminophosphonium carboxylate **119** formed and upon heating the amide formed.

It was determined that amidation is silane-mediated after monitoring a reaction between **119** and phenylsilane.  $^{31}\text{P}$  NMR revealed **119** was reduced to triphenylphosphine with some formation of **118** and  $\text{H}_2$ .  $^1\text{H}$  NMR showed no amide product, but there was some aminosilicon species **121** present (Figure 100). The experiment demonstrated that **119** is not an intermediate in amidation and the phosphine is not regenerated by reduction of triphenylphosphine oxide. After 15 hours at room temperature, the amide formed, and **121** disappeared, which suggests that silicon has a role in the amidation process.

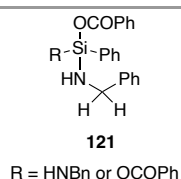


Figure 100 Benzylaminosilane species observed by NMR.

Andrews and Denton reacted phenylsilyl ester under the conditions of catalytic amidation and the amide product was observed in 64% yield. This means that the monophenylsilyl ester can mediate amidation with azide and triphenylphosphine. The authors propose an alternative mechanism for the Staudinger amidation (Figure 101). Initially, phosphorus-mediated azide reduction gives **122**, which is protonated by the carboxylic acid to give **119**. The carboxylate attacks the silane to initiate reduction of **119**, and this generates the silyl ester intermediate **123**, and **118**. A reaction between these allows for the regeneration of the phosphine catalyst and the aminosilyl ester **125** is formed leading to the amide and silanol and siloxane by-products. Their previous NMR experiments show that the silyl esters **124** and silamine species **125** are amide precursors. Here they describe an intramolecular C-N bond formation step. The authors emphasize that the silyl ester, which is generated *in situ*, is important because it acts as an activated carboxylic acid and as an enhanced reductant.

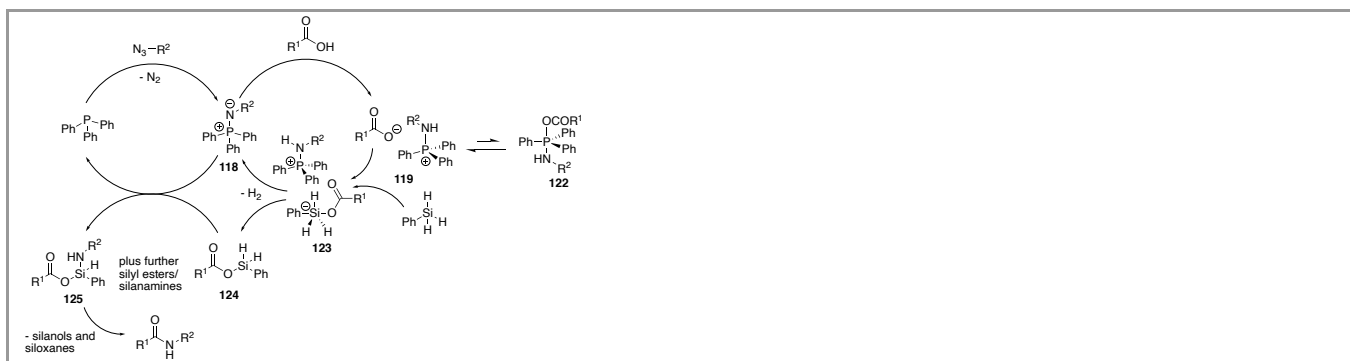
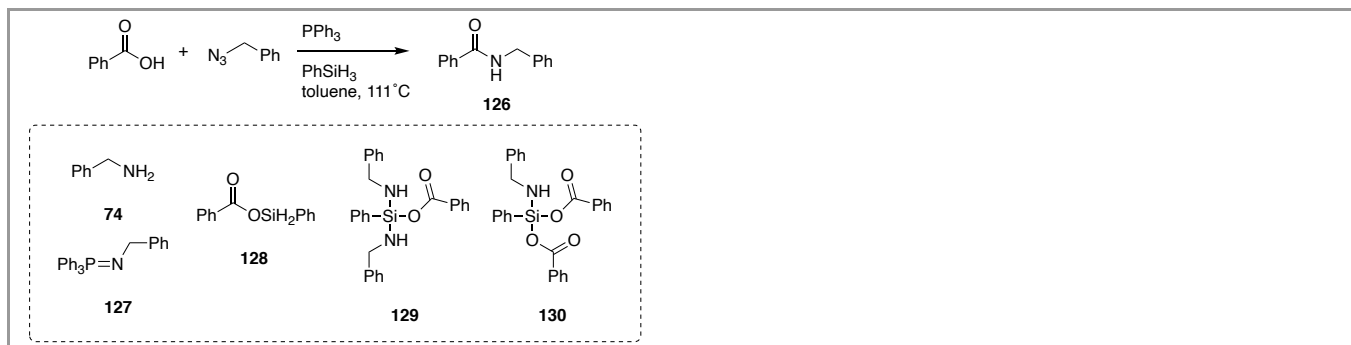


Figure 101 Proposed mechanism by Andrews and Denton for the catalytic Staudinger amidation.

White and Mecinović *et al.* further investigated the mechanism of the catalytic Staudinger amidation through various NMR

spectroscopy experiments.<sup>74</sup> Initially <sup>1</sup>H and <sup>31</sup>P NMR were used to perform a time-course experiment of the catalytic Staudinger ligation using benzoic acid and benzyl azide using triphenylphosphine and phenylsilane (Figure 102). NMR analysis revealed immediate formation of intermediates of benzylamine **74**, iminophosphorane **127**, silyl ester **128**, and benzylamine-containing species **129** and **130**. After 4 hours, the starting benzyl azide disappeared, and the amide product **126** was visible by NMR. **129** and **130** were still present after 4 hours, however, the amount of **129** increased. After 24 hours, there was increased formation of product **126**, and **127**, **129**, and **130** were no longer visible by NMR. Triphenylphosphine oxide was not produced over the course of the reaction (initially suggested by Ashfeld), and phenylsilane does not mediate the reduction of triphenylphosphine oxide to triphenylphosphine.



**Figure 102** Intermediates detected in the Staudinger amidation by White and Mecinović *et al.*

In order to understand the mechanism further, they first studied **129** and **130**, which immediately formed. Their presence was confirmed by 2D NMR analysis. <sup>1</sup>H NMR also revealed a minor species, which they speculated was a dimer. Further <sup>1</sup>H NMR analysis did reveal that the substituents on the silicon of **129** or **130** are the carboxylate or benzylamine. It was observed that the formation of amide product **126** was followed by the disappearance of **129** or **130**, so the authors looked to study this relationship. Exchange spectroscopy showed that **129** and **130** exchange with each other and free benzylamine. It was determined that **129** or **130** are off-cycle intermediates because when **129** or **130** are not present, amide formation occurs faster and these results suggest that they capture the reactive benzoic acid and benzylamine, essentially slowing the reaction.

The authors then wanted to investigate the role of the iminophosphorane **127** (Figure 103). The reaction of **127** with phenylsilane formed benzylamine (**74**) and triphenylphosphine as the only products (Figure 103a). **127** was protonated immediately upon the addition of benzoic acid, and in refluxing toluene it resulted in the slow formation of the amide (**126**) (Figure 103b). In the presence of phenylsilane, **127**<sup>+</sup> formed benzylamine **74** and triphenylphosphine, and subsequently formed the amide (Figure 103c). These reactions did not show the formation of **129** or **130** from **127**. Silyl ester **128** was another intermediate that formed in the beginning of the reaction. The authors were able to synthesize **128** and the reaction with **127** resulted in **129** and **130** in 55% and 45% yield, respectively (Figure 103d). The silyl ester was only able to form 40% of amide product when reacted with benzylamine **74** after 4 days. Lastly, they were able to complete stoichiometric phenylsilane-mediate amide coupling and they observed the amide in good yield, and the addition of catalytic triphenylphosphine or phosphine oxide did not negatively impact the reaction.

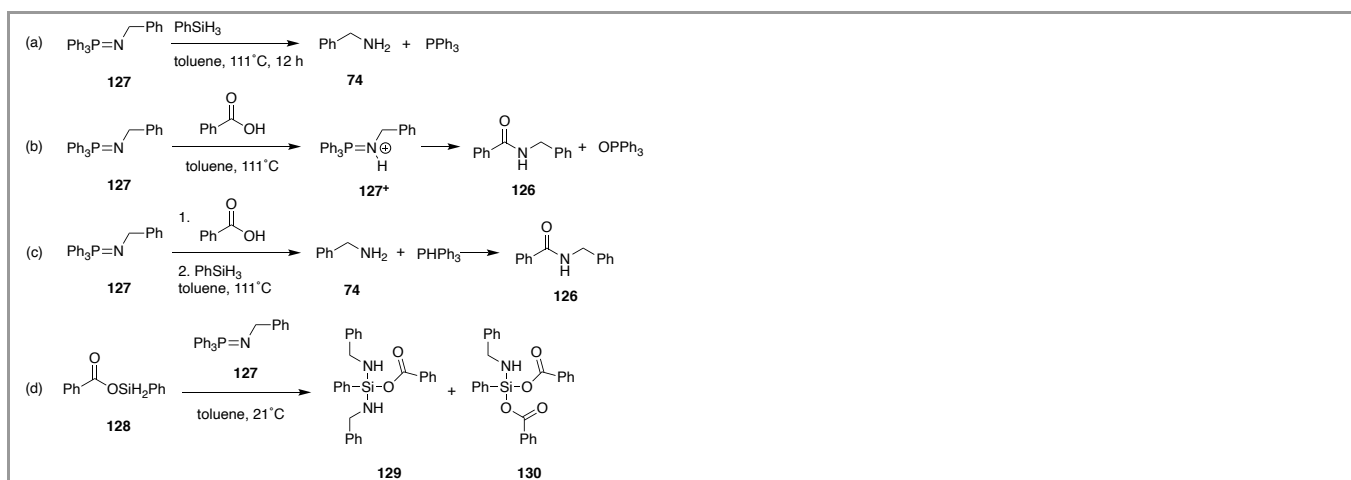


**Figure 103** Mechanistic experiments using **127**. (a) Reaction of **127** with phenylsilane. (b) Protonation of **127** and amide formation. (c) Formation of benzylamine from **127** and amide formation. (d) Formation of **129** and **130** from silyl ester **128**.

The authors then proposed a new catalytic cycle for the Staudinger ligation (Figure 104). First the benzyl azide reacts with triphenylphosphine to form **127**. Protonation by benzoic acid leads to **127**<sup>+</sup>. The reduction of **127**<sup>+</sup> by phenylsilane regenerates triphenylphosphine and gives benzylamine **72**. **72** is able to participate in different pathways: 1) it can react with benzoic acid and

phenylsilane to give amide **126**, 2) it can deprotonate benzoic acid, which can react with phenylsilane to produce silyl ester **128**, and **128** can react further with **127** to give the off-cycle silylbenzylamine intermediates **129** and **130**, and 3) **74** can participate in an equilibrium with **129** and **130** causing the slow release of benzoic acid. The benzoic acid and benzylamine can then react to form the amide with any remaining phenylsilane.

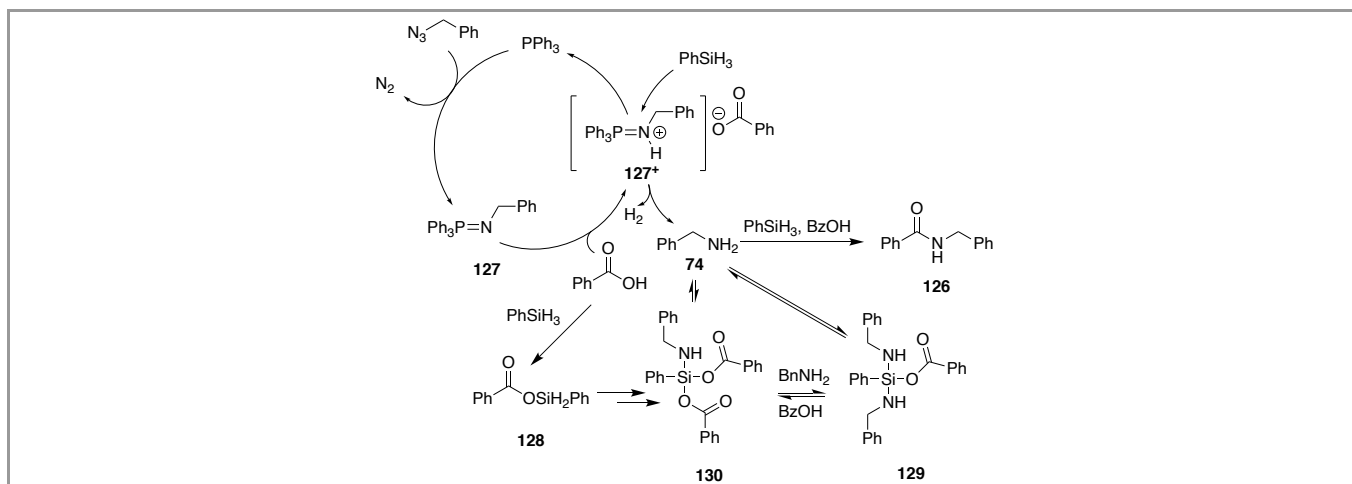


**Figure 104** Proposed catalytic cycle for the Staudinger ligation by White and Mecinović *et al.*

As another example, we examine a catalytic process in which phenylsilane is employed as a terminal reductant in the presence of a Bronsted acid and a base, and outline clues as to the possible intervention of *in situ*-generated silyl esters. O'Brien and co-workers have pioneered the development of the catalytic Wittig reaction in which phenyl- and diphenylsilane are employed as terminal reductants. The silanes are pivotal to these catalytic reactions since, to achieve turnover, a phosphine oxide must be reduced to a phosphine in the presence of other reducible functional groups such as aldehydes and alkenes. Depicted in Figure 105 is O'Brien's original catalytic Wittig protocol<sup>101</sup> (a) along with a remarkable room-temperature catalytic Wittig reaction (b).<sup>102</sup> In both cases the catalytic cycle is close by silane-mediated phosphine oxide reduction which constitutes the turnover-limiting step (Figure 105c). The room temperature protocol is made possible by the addition of substoichiometric *para*-nitrobenzoic acid and the significant rate acceleration was attributed to "proton activation" of the phosphine oxide which renders it more electrophilic thereby promoting hydride transfer from the silane.

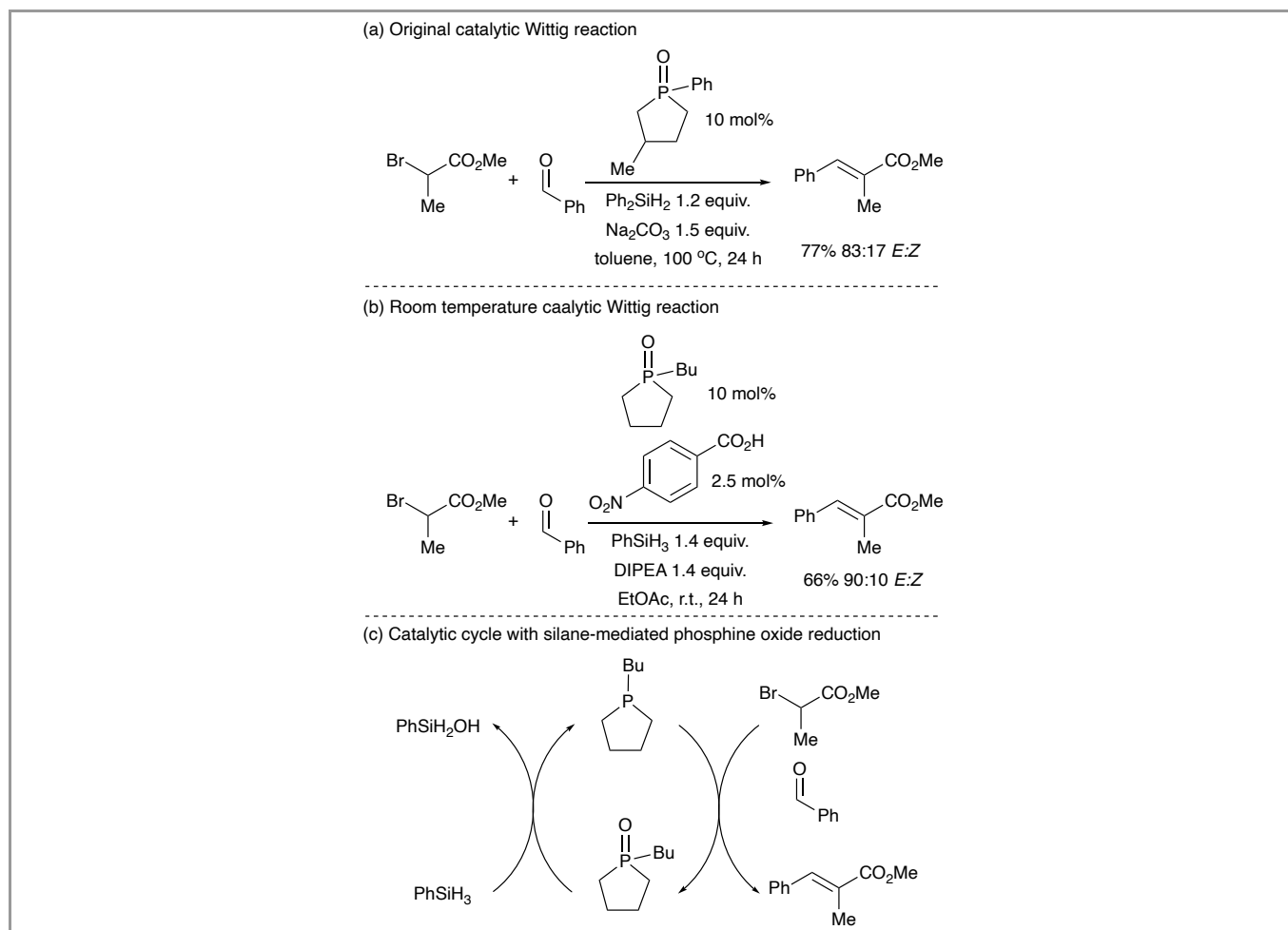


**Figure 105** The remarkable effect of a Brønsted acid additive in the catalytic Wittig reaction.

However, O'Brien and co-workers have demonstrated that enhanced phosphine oxide reduction is not just contingent upon the presence of *para*-nitrobenzoic acid (Table 1). In the presence of the carboxylic acid alone no reaction occurs (entry 3, Table 1). Given that silyl esters are known to form rapidly from phenylsilane and carboxylic acids in the presence of tertiary amines (see Section 3.5, Figure 40) it is possible that they are formed *in situ* in the catalytic Wittig reaction.

**Table 1** The dependence of the enhanced reduction on the presence of Hünig's base.<sup>a</sup>

Entry	DIPEA (equiv.)	Acid (equiv.)	Conversion (%)
1	14.0	1.0	61
2	14.0	-	6
3	-	1.0	0

<sup>a</sup>The same reactivity pattern was observed under various conditions, using both PhSiH<sub>3</sub> and Ph<sub>2</sub>SiH<sub>2</sub> and with different phosphine oxides.



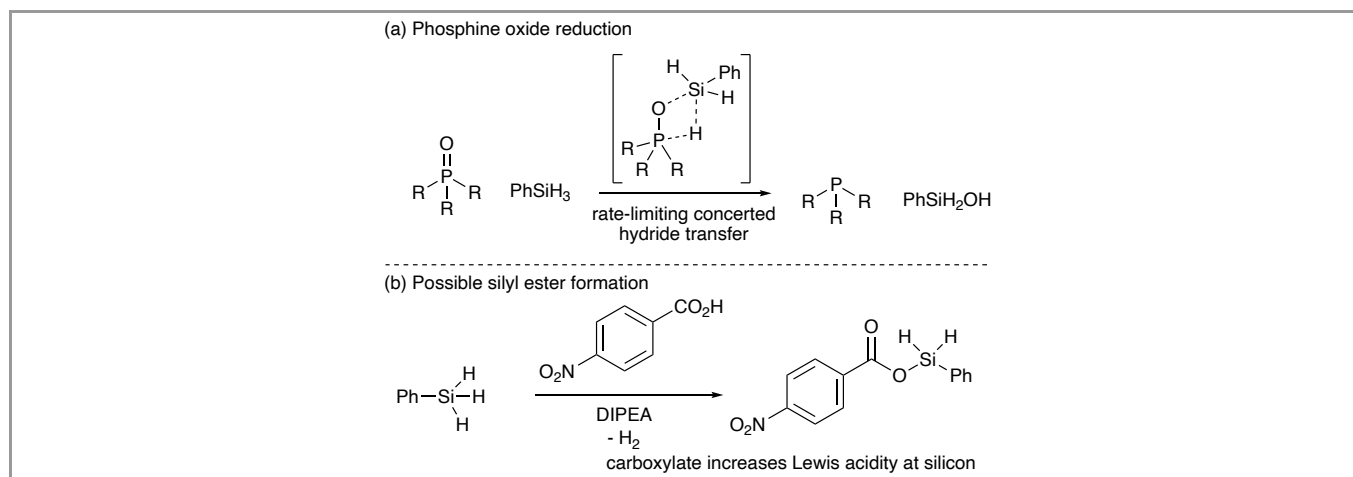


**Figure 106** (a) The cyclic and concerted nature of the rate-limiting hydride transfer step in hydrosilane-mediated phosphine oxide reduction. (b) The possible generation of a Lewis acidic silyl ester from phenyl silane and nitrobenzoic acid.

In this review, we have outlined the increasing Lewis acidity of silyl esters compared their parent silanes. This understanding prompts a stronger alternative hypothesis to the role of the Bronsted acid, when combined with knowledge of phosphine oxide chemistry. The “protic” role of the Bronsted acid, suggested by the authors, is centered around *increasing* electrophilicity at phosphorus and is not congruous with published experimental (Figure 105) and computational data.<sup>103</sup> The mechanism of silane-mediated phosphine oxide reduction was also examined computationally by Kenske and O'Brien in 2020. This important study established that the rate limiting step of the reduction process was hydride transfer from the silane reductant to the phosphine oxide (Figure 106). Moreover, the computed transition structure for this process is cyclic and concerted and characterised by simultaneous phosphorus-hydrogen and oxygen silicon bond-making (Figure 106a). Such a transition state geometry is key in explaining the somewhat counterintuitive experimental fact that electron rich (more Lewis basic) phosphine oxides are reduced much more rapidly by hydrosilanes than their electron deficient counterparts. These experimental facts are not consistent with proton activation since complete (or partial) protonation of the phosphine oxide will significantly reduce the Lewis basicity of the phosphoryl oxygen. As a corollary, increasing Lewis acidity at silicon by replacing hydrogens in phenylsilane with electron withdrawing carboxylates through silyl ester formation ought to accelerate reduction for the same reason. Therefore, a potential, but as yet untested, alternative explanation for the role of nitrobenzoic acid in the room temperature Wittig reaction could be formation of silyl esters which contain activating carboxylate groups resulting in a more electron deficient and Lewis acidic silicon which facilitates hydride transfer (Figure 106b). While experimental studies are required to establish specific mechanistic detail in this system, it is clear that the potential for *in situ* silyl ester formation exists and that their intervention offers an alternative explanation that is in agreement with extant experimental and computational data.

We leave this hypothesis as an example of how the appreciation and understanding of the reactivity of silyl ester, as has been highlighted in the previous sections of this review, should lead to the design of improved silane-mediated catalytic reactions.

## 9. Conclusion

A variety of activated carboxylic acid derivatives have long been recognized as useful reactive intermediates in organic synthesis. Acid chlorides, anhydrides, and coupling-agent-activated acids are the most prominent, and each has their own benefits and detriments. While silyl esters are not generally thought of as readily accessible activated carboxylic acid derivatives, this review demonstrates that 1) such intermediates have indeed been used widely in organic synthesis and 2) their potential for use and opportunity for innovation in this arena are great. The field of silicon reagents and catalysts in organic synthesis is undergoing a renaissance due to their green-ness and practicality, and we envision a bright future for such endeavours as the unique and useful reactivity of organosilanes continues to be explored in the modern day.

## Funding Information

[Click here to insert sources of funding, grant numbers, etc. Do not repeat the same in the acknowledgment.](#)

## Acknowledgment

[Click here to insert acknowledgment text. Funding sources and grant numbers should be given above in the Funding Information section.](#)

## Conflict of Interest

The authors declare no conflict of interest.

## References

- (1) Yur'ev, Y. K.; Belyakova, Z. V. *Russian Chem. Rev.* **1960**, 29 (7), 383–394.

- 
- (2) Wuts, P. G. M.; Greene, T. W. Protection for the Carboxyl Group. In *Greene's Protective Groups in Organic Synthesis*; John Wiley & Sons, Inc., 2014; pp 533–646.
- (3) Combs, J. R.; Lai, Y. C.; Van Vranken, D. L. *Org. Lett.* **2021**, *23* (8), 2841–2845.
- (4) Fujita, T.; Yamane, M.; Ameera, W. M. C. S.; Mitsunuma, H.; Kanai, M. *Angew. Chem. Int. Ed.* **2021**, *60* (46), 24598–24604.
- (5) Hudrlik, P. F.; Feasley, R. *Tetrahedron Lett.* **1972**, 1781–1784.
- (6) Weinberg, J. M.; Gitto, S. P.; Wooley, K. L. *Macromolecules* **1998**, *31* (1), 15–21.
- (7) Wang, M.; Gan, D.; Wooley, K. L. *Macromolecules* **2001**, *34* (10), 3215–3223.
- (8) Wang, M.; Weinberg, J. M.; Wooley, K. L. *Macromolecules* **1998**, *31* (22), 7606–7612.
- (9) Gitto, S. P.; Wooley, K. L. *Macromolecules* **1995**, *28* (26), 8887–8889.
- (10) (a) Muramatsu, W.; Yamamoto, H. *J. Am. Chem. Soc.* **2019**, *141* (48), 18926–18931. (b) Muramatsu, W.; Hattori, T.; Yamamoto, H. *J. Am. Chem. Soc.* **2019**, *141* (31), 12288–12295.
- (11) Kagiya, T.; Sumida, Y.; Tachi, T. *Bull. Chem. Soc. Japan* **1970**, *43* (12), 3716–3722.
- (12) Silyl esters have also been accessed through esters and anhydrides: (a) Mbah, G. C.; Speier, J. L. *J. Organomet. Chem.* **1984**, *271* (1–3), 77–82. (b) Sauer, R. O.; Patnode, W. *J. Am. Chem. Soc.* **1945**, *67*, 1548–1549. (c) Schuyten, H. A.; Weaver, J. W.; David Reid, J. *J. Am. Chem. Soc.* **1947**, *69*, 2110–2112. (d) Post, H. W.; Hofrichter Jr., C. H. *J. Org. Chem.* **1940**, *5*, 443–448. (e) Friedel, C.; Ladenburg, A. *Justus Liebigs Ann. Chem.* **1868**, *145* (2), 174–178.
- (13) Aizpurua, J. M.; Palomo, C. *Can. J. Chem.* **1984**, *62*, 336–340.
- (14) Palomo, C. *Synthesis* **1981**, 1981 (10), 809–811.
- (15) Jereb, M.; Lakner, J. *Tetrahedron* **2016**, *72* (37), 5713–5723.
- (16) Chauhan, M.; Chauhan, B. P. S.; Boudjouk, P. *Org. Lett.* **2000**, *2* (8), 1027–1029.
- (17) Liu, G. B.; Zhao, H. Y.; Thiemann, T. *Synth. Commun.* **2007**, *37* (16), 2717–2727.
- (18) Liu, G. B. *Synlett* **2006**, 2006 (9), 1431–1433.
- (19) Schubert, U.; Lorenz, C. *Inorg. Chem.* **1997**, *36* (6), 1258–1259.
- (20) Julián, A.; Garcés, K.; Lalrempuia, R.; Jaseer, E. A.; García-Orduña, P.; Fernández-Alvarez, F. J.; Lahoz, F. J.; Oro, L. A. *ChemCatChem* **2018**, *10* (5), 1027–1034.
- (21) Vijjamarr, S.; Chidara, V. K.; Rousova, J.; Du, G. *Catal. Sci. Technol.* **2016**, *6* (11), 3886–3892.
- (22) Liu, G. Bin; Zhao, H. Y.; Thiemann, T. *Adv. Synth. Catal.* **2007**, *349* (6), 807–811.
- (23) Ojima, Y.; Yamaguchi, K.; Mizuno, N. *Adv. Synth. Catal.* **2009**, *351* (9), 1405–1411.
- (24) Stoll, E. L.; Tongue, T.; Andrews, K. G.; Valette, D.; Hirst, D. J.; Denton, R. M. *Chem. Sci.* **2020**, *11* (35), 9494–9500.
- (25) Morisset, E.; Chardon, A.; Rouden, J.; Blanchet, J. *European J. Org. Chem.* **2020**, 2020 (3), 388–392.
- (26) Sayes, M.; Charette, A. B. *Green Chem.* **2017**, *19* (21), 5060–5064.
- (27) Niu, H.; Lu, L.; Shi, R.; Chiang, C. W.; Lei, A. *Chem. Commun.* **2017**, 53 (6), 1148–1151.
- (28) Rauch, M.; Strater, Z.; Parkin, G. *J. Am. Chem. Soc.* **2019**, *141* (44), 17754–17762.
- (29) Hulla, M.; Nussbaum, S.; Bonnin, A. R.; Dyson, P. J. *Chem. Commun.* **2019**, 55 (87), 13089–13092.
- (30) Fernández-Alvarez, F. J.; Aitani, A. M.; Oro, L. A. *Catal. Sci. Technol.* **2014**, *4* (3), 611–624.
- (31) Fernández-Alvarez, F. J.; Oro, L. A. *ChemCatChem* **2018**, *10* (21), 4783–4796.
- (32) Chen, J.; McGraw, M.; Chen, E. Y. X. *ChemSusChem* **2019**, *12* (20), 4543–4569.
- (33) Li, Y.; Cui, X.; Dong, K.; Junge, K.; Beller, M. *ACS Catal.* **2017**, *7* (2), 1077–1086.
- (34) Motokura, K.; Kashiwame, D.; Takahashi, N.; Miyaji, A.; Baba, T. *Chemistry - A European Journal* **2013**, *19* (30), 10030–10037.
- (35) Fang, C.; Lu, C.; Liu, M.; Zhu, Y.; Fu, Y.; Lin, B. L. *ACS Catal.* **2016**, *6* (11), 7876–7881.
- (36) Motokura, K.; Naijo, M.; Yamaguchi, S.; Miyaji, A.; Baba, T. *Chem. Lett.* **2015**, *44* (9), 1217–1219.
- (37) Itagaki, S.; Yamaguchi, K.; Mizuno, N. *J. Mol. Catal. A Chem.* **2013**, *366* (2013), 347–352.
- (38) Hulla, M.; Laurency, G.; Dyson, P. J. *ACS Catal.* **2018**, *8* (11), 10619–10630.
- (39) Murata, T.; Hiyoshi, M.; Ratanasak, M.; Hasegawa, J. Y.; Ema, T. *Chem. Commun.* **2020**, 56 (43), 5783–5786.
- (40) Jacquet, O.; Das Neves Gomes, C.; Ephritikhine, M.; Cantat, T. *J. Am. Chem. Soc.* **2012**, *134* (6), 2934–2937.
- (41) Frogneux, X.; Jacquet, O.; Cantat, T. *Catal. Sci. Technol.* **2014**, *4* (6), 1529–1533.
- (42) Bryan, M. C.; Dunn, P. J.; Entwistle, D.; Gallou, F.; Koenig, S. G.; Hayler, J. D.; Hickey, M. R.; Hughes, S.; Kopach, M. E.; Moine, G.; Richardson, P.; Roschangar, F.; Steven, A.; Weiberth, F. J. *Green Chem.* **2018**, *20* (22), 5082–5103.
- (43) Davies, J. J.; Braddock, D. C.; Lickiss, P. D. *Org. Biomol. Chem.* **2021**, *19* (31), 6746–6760.
- (44) McKnelly, K. J.; Sokol, W.; Nowick, J. S. *J. Org. Chem.* **2020**, *85* (3), 1764–1768.
- (45) Hollanders, K.; Maes, B. U. W.; Ballet, S. *Synthesis* **2019**, 51, 2261–2277.
- (46) Pattabiraman, V. R.; Bode, J. W. *Nature* **2011**, *480* (7378), 471–479.
- (47) Wang, K.; Lu, Y.; Ishihara, K. *Chem. Commun.* **2018**, 54 (43), 5410–5413.
- (48) Liu, S.; Yang, Y.; Liu, X.; Ferdousi, F. K.; Batsanov, A. S.; Whiting, A. *European J. Org. Chem.* **2013**, 2013 (25), 5692–5700.
- (49) Ishihara, K.; Ohara, S.; Yamamoto, H. *J. Org. Chem.* **1996**, *61* (13), 4196–4197.
- (50) Gernigon, N.; Al-Zoubi, R. M.; Hall, D. G. *J. Org. Chem.* **2012**, *77* (19), 8386–8400.
- (51) Al-Zoubi, R. M.; Marion, O.; Hall, D. G. *Angew. Chem. Int. Ed.* **2008**, *47* (15), 2876–2879.
- (52) Sabatini, M. T.; Boulton, L. T.; Sheppard, T. D. *Sci. Adv.* **2017**, *3* (9), 1–8.
- (53) Coomber, C. E.; Laserna, V.; Martin, L. T.; Smith, P. D.; Hailes, H. C.; Porter, M. J.; Sheppard, T. D. *Org. Biomol. Chem.* **2019**, *17* (26), 6465–6469.
- (54) De Figueiredo, R. M.; Suppo, J. S.; Campagne, J. M. *Chem. Rev.* **2016**, *116* (19), 12029–12122.
- (55) Sabatini, M. T.; Boulton, L. T.; Sneddon, H. F.; Sheppard, T. D. *Nat. Catal.* **2019**, *2* (1), 10–17.
- (56) Chan, T. H.; Wong, L. T. L. *J. Org. Chem.* **1969**, *34* (9), 2766–2767.
- (57) Chan, T. H.; Wong, L. T. L. *J. Org. Chem.* **1971**, *36* (6), 850–853.
- (58) Van Leeuwen, S. H.; Quaedflieg, P. J. L. M.; Broxterman, Q. B.; Liskamp, R. M. J. *Tetrahedron Lett.* **2002**, *43* (50), 9203–9207.
- (59) Nobuta, T.; Morishita, H.; Suto, Y.; Yamagiwa, N. *Synlett* **2022**, 33 (15), 1563–1569.
- (60) Aspin, S. J.; Taillemaud, S.; Cyr, P.; Charette, A. B. *Angew. Chem. Int. Ed.* **2016**, *128* (44), 14037–14041.
- (61) Chou, W. C.; Chou, M. C.; Lu, Y. Y.; Chen, S. F. *Tetrahedron Lett.* **1999**, *40* (17), 3419–3422.
- (62) Tozawa, T.; Yamane, Y.; Mukaiyama, T. *Chem. Lett.* **2005**, *34* (5), 734–735.
- (63) Tozawa, T.; Yamane, Y.; Mukaiyama, T. *Chem. Lett.* **2005**, *34* (10), 1334–1335.
- (64) Tozawa, T.; Yamane, Y.; Mukaiyama, T. *Chem. Lett.* **2005**, *34* (12), 1586–1587.
-

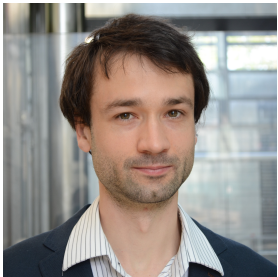
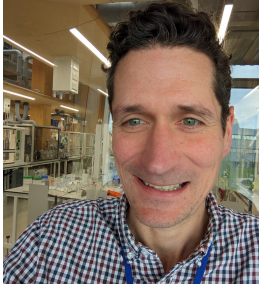

- (65) Tozawa, T.; Yamane, Y.; Mukaiyama, T. *Heterocycles* **2006**, *67* (2), 629–641.
- (66) Braddock, D. C.; Lickiss, P. D.; Rowley, B. C.; Pugh, D.; Purnomo, T.; Santhakumar, G.; Fussell, S. J. *Org. Lett.* **2018**, *20* (4), 950–953.
- (67) Braddock, D. C.; Davies, J. J.; Lickiss, P. D. *Org. Lett.* **2022**, *24* (5), 1175–1179.
- (68) Lainer, T.; Czerny, F.; Haas, M. *Org. Biomol. Chem.* **2022**, *20* (18), 3717–3720.
- (69) Muramatsu, W.; Manthena, C.; Nakashima, E.; Yamamoto, H. *ACS Catal.* **2020**, *10* (16), 9594–9603.
- (70) Muramatsu, W.; Yamamoto, H. *Org. Lett.* **2022**, *24* (39), 7194–7199.
- (71) Ruan, Z.; Lawrence, R. M.; Cooper, C. B. *Tetrahedron Lett.* **2006**, *47* (43), 7649–7651.
- (72) Kosal, A. D.; Wilson, E. E.; Ashfeld, B. L. *Angew. Chem. Int. Ed.* **2012**, *51* (48), 12036–12040.
- (73) Andrews, K. G.; Denton, R. M. *Chem. Commun.* **2017**, *53* (57), 7982–7985.
- (74) White, P. B.; Rijpkema, S. J.; Bunschoten, R. P.; Mecinović, J. *Org. Lett.* **2019**, *21* (4), 1011–1014.
- (75) D’Amaral, M. C.; Jamkhou, N.; Adler, M. J. *Green Chem.* **2021**, *23* (1), 288–295.
- (76) Andrews, K. G.; Summers, D. M.; Donnelly, L. J.; Denton, R. M. *Chem. Commun.* **2016**, *52* (9), 1855–1858.
- (77) Cheng, C.; Brookhart, M. J. *Am. Chem. Soc.* **2012**, *134* (28), 11304–11307.
- (78) Krysin, E. P.; Karel, V. N.; Antonov, A. A.; Rostovskaya, G. E. *Chem. Nat. Compd.* **1979**, *15*, 601–603.
- (79) Jiang, Y. Y.; Zhu, L.; Liang, Y.; Man, X.; Bi, S. J. *Org. Chem.* **2017**, *82* (17), 9087–9096.
- (80) Hu, B.; Jiang, Y. Y.; Liu, P.; Zhang, R. X.; Zhang, Q.; Liu, T. T.; Bi, S. *Org. Biomol. Chem.* **2019**, *17* (41), 9232–9242.
- (81) From ref. 76: “Geometry Optimization Was Conducted with TheωB97X-D Method, Def2-SVP Basis Set and SMD Solvation Model (Solvent = Acetonitrile).”
- (82) Gevorgyan, V.; Rubin, M.; Liu, J. X.; Yamamoto, Y. *J. Org. Chem.* **2001**, *66* (5), 1672–1675.
- (83) Bézier, D.; Park, S.; Brookhart, M. *Org. Lett.* **2013**, *15* (3), 496–499.
- (84) Corriu, R. J. P.; Lanneau, G. F.; Perrot, M. *Tetrahedron Lett.* **1987**, *28* (34), 3941–3944.
- (85) Andrews, K. G.; Faizova, R.; Denton, R. M. *Nat. Commun.* **2017**, *8*, 1–6.
- (86) Venkateswaran, P. S.; Bardos, T. J. *J. Org. Chem.* **1967**, *32* (4), 1256–1257.
- (87) Chandrasekhar, S.; Kumar, M. S.; Muralidhar, B. *Tetrahedron Lett.* **1998**, *39* (8), 909–910.
- (88) Matsubara, K.; Iura, T.; Maki, T.; Nagashima, H. *J. Org. Chem.* **2002**, *67* (14), 4985–4988.
- (89) Miyamoto, K.; Motoyama, Y.; Nagashima, H. *Chem. Lett.* **2012**, *41* (3), 229–231.
- (90) Fernández-Salas, J. A.; Manzini, S.; Nolan, S. P. *Adv. Synth. Catal.* **2014**, *356* (2–3), 308–312.
- (91) Castro, L. C. M.; Li, H.; Sortais, J. B.; Darcel, C. *Chem. Commun.* **2012**, *48* (85), 10514–10516.
- (92) Zheng, J.; Chevance, S.; Darcel, C.; Sortais, J. B. *Chem. Commun.* **2013**, *49* (85), 10010–10012.
- (93) Antico, E.; Schlichter, P.; Werlé, C.; Leitner, W. *J. Am. Chem. Soc.* **2021**, *143* (6), 742–749.
- (94) Wei, D.; Buhaibeh, R.; Canac, Y.; Sortais, J. B. *Org. Lett.* **2019**, *21* (19), 7713–7716.
- (95) Bajracharya, G. B.; Nogami, T.; Jin, T.; Matsuda, K.; Gevorgyan, V.; Yamamoto, Y. *Synthesis* **2004**, *2004* (2), 308–311.
- (96) Nimmagadda, R. D.; McRae, C. *Tetrahedron Lett.* **2006**, *47* (21), 3505–3508.
- (97) Stoll, E. L.; Barber, T.; Hirst, D. J.; Denton, R. M. *Chem. Commun.* **2022**, *58* (21), 3509–3512.
- (98) Wissner, A.; Grudzinskas, C. V. *J. Org. Chem.* **1978**, *43* (20), 3972–3974.
- (99) (a) Kosal, A. D.; Wilson, E. E.; Ashfeld, B. L. *Angew. Chem. Int. Ed.* **2012**, *51*, 12036–12040. (b) O’Brien, C. J.; Tellez, J. L.; Nixon, Z. S.; Kang, L. J.; Carter, A. L.; Kunkel, S. R.; Przeworski, K. C.; Chass, G. A. *Angew. Chem. Int. Ed.* **2009**, *48*, 6836–6839. (c) O’Brien, C. J.; Lavigne, F.; Coyle, E. E.; Holohan, A. J.; Doonan, B. J. *Chem. Eur. J.* **2013**, *19*, 5854–5858. (d) Handoko; Panigrahi, N. R.; Arora, P. S. *J. Am. Chem. Soc.* **2022**, *144* (8), 3637–3643. (e) Lipshultz, J. M.; Radosevich, A. T. *J. Am. Chem. Soc.* **2021**, *143*, 14487–14494. (f) Lecomte, M.; Lipshultz, J. M.; Kim-Lee, S. H.; Li, G.; Radosevich, A. T. *J. Am. Chem. Soc.* **2019**, *141*, 12507–12512. (g) Wang, A.; Xie, Y.; Wang, J.; Shi, D.; Yu, H. *Chem. Commun.* **2022**, *58*, 1127–1130. (h) Wei, D.; Netkaew, C.; Darcel, C. *Adv. Synth. Catal.* **2019**, *361*, 1781–1786. (i) Liu, Z.; Wu, C.; Luo, X.; Zhang, H.; Liu, X.; Ji, G.; Liu, Z. *Green Chem.* **2017**, *19*, 3525–3529. (j) Ogiwara, Y.; Uchiyama, T.; Sakai, N. *Angew. Chem. Int. Ed.* **2016**, *55*, 1864–1867. (k) Wang, T.; Xu, H.; He, J.; Zhang, Y. *Tetrahedron* **2020**, *76*, 131394. (l) Sorribes, I.; Junge, K.; Beller, M. *J. Am. Chem. Soc.* **2014**, *136* (40), 14314–14319. (m) Fu, M. C.; Shang, R.; Cheng, W. M.; Fu, Y. *Angew. Chem. Int. Ed.* **2015**, *54*, 9042–9046. (n) Nguyen, T. V. Q.; Yoo, W. J.; Kobayashi, S. *Adv. Synth. Catal.* **2016**, *358*, 452–458. (o) Huang, D. W.; Liu, Y. H.; Peng, S. M.; Liu, S. T. *Dalt. Trans.* **2016**, *45*, 8265–8271. (p) Fernández-Salas, J. A.; Manzini, S.; Nolan, S. P. *Adv. Synth. Catal.* **2014**, *356*, 308–312. (q) Antico, E.; Schlichter, P.; Werlé, C.; Leitner, W. *J. Am. Chem. Soc.* **2021**, *143*, 742–749. (r) Bhunia, M.; Sahoo, S. R.; Shaw, B. K.; Vaidya, S.; Pariyar, A.; Vijaykumar, G.; Adhikari, D.; Mandal, S. K. *Chem. Sci.* **2019**, *10*, 7433–7441.
- (100) Garcia, J.; Urpí, F.; Vilarrasa, J. *Tetrahedron Lett.* **1984**, *25* (42), 4841–4844.
- (101) O’Brien, C. J.; Tellez, J. L.; Nixon, Z. S.; Kang, L. J.; Carter, A. L.; Kunkel, S. R.; Przeworski, K. C.; Chass, G. A. *Angew. Chem. Int. Ed.* **2009**, *48* (37), 6836–6839.
- (102) O’Brien, C. J.; Lavigne, F.; Coyle, E. E.; Holohan, A. J.; Doonan, B. J. *Chemistry - A European Journal* **2013**, *19* (19), 5854–5858.
- (103) Kirk, A. M.; O’Brien, C. J.; Krenske, E. H. *Chem. Commun.* **2020**, *56* (8), 1227–1230.

## Biosketches



Melissa C. D’Amaral is a research assistant in the Department of Chemistry and Biology at Toronto Metropolitan University (Canada). She received her BSc in Chemistry and MSc in Molecular Science at Toronto Metropolitan University in 2020 and 2022, respectively, and completed her theses under the guidance of Prof. Marc J. Adler. When not working, she loves spending time with friends and family, and playing volleyball.

---

	<p>Keith Andrews is currently an 1851 Research Fellow at the University of Oxford. He obtained his PhD with Professor Ross Denton at the University of Nottingham before joining the laboratory of Professor Harry L. Anderson FRS at the University of Oxford to carry out postdoctoral research.</p>
	<p>Ross M. Denton is a Professor of Organic Chemistry based in the GlaxoSmithKline Laboratory for Sustainable Chemistry within the School of Chemistry at the University of Nottingham (UK). He obtained his PhD degree at the University of Nottingham before carrying out postdoctoral research at the Scripps Research Institute in La Jolla (USA) and the University of Cambridge (UK). He began his independent academic career at the University of Nottingham in 2008 as an Assistant Professor and was promoted to full Professor in 2020. He is the recipient of the 2020 SCI Process Chemistry Award and the 2022 Royal Society of Chemistry Bader Prize.</p>
	<p>Marc J. Adler is an Associate Professor in the Department of Chemistry &amp; Biology at Toronto Metropolitan University (Canada). He was born in San Diego, CA (USA), received degrees in chemistry from University of California, Berkeley (USA, BSc) and Duke University (USA, Ph.D.), and further trained as a postdoctoral researcher at Yale University (USA) and University of Oxford (UK). He began his independent academic career at Northern Illinois University (USA). He loves family and friends, and lives by the motto “stay far from timid, only make moves when your heart’s in it, and live the phrase ‘sky’s the limit’” (Christopher Wallace).</p>

---